„ALEXANDRU IOAN CUZA" UNIVERSITY OF IASI
FACULTY OF BIOLOGY
DOCTORAL SCHOOL OF BIOLOGY

EVALUATION OF THE BIOTECHNOLOGICAL POTENTIAL OF *BACILLUS SAFENSIS* P1.5S AND *BACILLUS VELEZENSIS* P3.3S STRAINS UNDER ABIOTIC STRESS CONDITIONS USING FUNCTIONAL AND GENOMIC ANALYSES

Summary of the doctoral thesis

Scientific advisor,
Prof. PhD habil. Marius STEFAN

PhD student,
Loredana-Elena MANTEA

Iasi, 2025

TABLE OF CONTENTS

INTRODUCTION

Agriculture is one of the most important economic sectors, playing an essential role in ensuring global food security. According to United Nations estimates, the world population will reach approximately 9.7 billion by 2050, which will require an increase in food production of up to 70% in order to meet the growing demand for food (United Nations, 2019; Kumar *et al*., 2021). This challenge is intensified by climate change, considered one of the most serious global problems with a direct impact on sustainable agriculture (World Bank, 2021). Associated effects, such as rising average temperatures, droughts, extreme weather events, sea level rise, and high carbon dioxide concentrations, negatively affect both the quantity and quality of agricultural production, hampering efforts to ensure sufficient and healthy food for the growing human population (Kumar *et al*., 2021).

Climate change has already had a noticeable impact on global food production, with productivity and estimated yields of major staple crops declining in all regions of the world (Arora, 2019; Ray *et al*., 2019). Furthermore, according to the Intergovernmental Panel on Climate Change, by the end of the 21st century, significant areas of fertile agricultural land are expected to be lost or degraded due to negative climate effects (Calvin *et al*., 2023). Another important impact of these changes is the decrease in the availability of essential nutrients in the soil, which further contributes to the decline in the efficiency of agricultural systems (Haque *et al*., 2020). Phosphorus (P) is one of the most important macronutrients, being essential for plant growth and development (Wan *et al*., 2020). However, due to its low solubility, P availability can be limited in many soils, with significant effects on plant growth and agricultural productivity. In addition to nutrient deficiencies, biotic stress generated by climate change-through the intensification of invasive weeds, pests, and diseases-exacerbates pressures on agri-food production, affecting its stability and sustainability (Haque *et al*., 2020). In this context, modern agriculture has focused primarily on the intensive use of chemical fertilizers and pesticides to increase crop yields (Cao *et al*., 2018). However, the uncontrolled and excessive application of these agrochemicals have had serious consequences for the environment, including soil and water pollution and the degradation of natural ecosystems. In response to these challenges, the agriculture of the future proposes sustainable solutions, among which the use of beneficial microorganisms stands out. These can act as both biofertilizers and biopesticides, contributing to improving soil fertility, mobilizing essential nutrients, increasing plant resistance to abiotic stress induced by climate change, and combating phytopathogenic agents and diseases affecting agricultural crops (Ali and Glick, 2019).

Root-associated bacteria play an essential role in promoting plant growth and alleviating stress through direct and indirect mechanisms of action. Direct mechanisms refer to increased nutrient uptake through nitrogen fixation, phosphorus solubilization, and the secretion of siderophores, phytohormones, or the production of 1-aminocyclopropane-1-carboxylate deaminase, as well as the

induction of systemic resistance. Indirect mechanisms are mediated by the suppression of phytopathogenic agents through the production of antimicrobial substances, lytic enzymes, and competition for ecological niche colonization (Sun *et al*., 2022).

The effectiveness of plant growth-promoting bacteria can be influenced by climate change. Therefore, bacterial strains used in agriculture should have a high tolerance to abiotic stress (such as salinity, drought, extreme temperatures, pH variations) in order to be effectively applied in soils affected by climate change. At the same time, the manifestation of beneficial effects on plants is conditioned by the efficient colonization of plant roots under stress conditions. Colonization is a complex process involving a number of mechanisms: chemotaxis (orientation based on chemical signals emitted by the root), motility (ability to move), quorum sensing (bacterial intercellular communication), and biofilm formation (Dong *et al*., 2022). In the context of climate change, bacteria that can stimulate plant growth and are tolerant to abiotic stress may represent a sustainable and effective alternative for modern agriculture. Bacteria associated with the rhizosphere can ensure optimal plant growth under stressful conditions through mechanisms such as phosphorus solubilization and control of phytopathogenic agents. A deeper understanding of these processes is essential to ensure sustainable agricultural production in the context of climate change.

The continuous growth of the global population requires finding sustainable solutions that maintain agricultural productivity and ensure the ever-increasing demand for food, despite the negative effects of climate change. The use of abiotic stress-tolerant rhizosphere bacteria may be a possible solution for stimulating plant growth under unfavorable conditions, thus contributing to food security in an increasingly unstable agricultural context.

SCOPE AND OBJECTIVES

The aim of this study was to evaluate, under abiotic stress conditions, the mechanisms involved in stimulating plant growth, present in two bacterial strains belonging to the *Bacillus* genus. To this end, functional and genomic approaches were used to establish the biotechnological potential of the investigated strains. To achieve this goal, six main objectives were formulated, each with specific associated activities:

1. Screening of bacterial strains with potential to stimulate plant growth

1.1. Isolation and characterization of phosphate solubilizing bacteria

1.2. Assessment of the tricalcium phosphate–solubilizing potential of the isolated bacterial strains

1.3. Investigation of the mechanisms involved in tricalcium phosphate solubilization

1.4. Detection of indole-3-acetic acid (IAA) production

1.5. Assessment of the production capacity of 1-aminocyclopropane-1-carboxylate (ACC) deaminase

1.6. Evaluation of the antifungal activity of bacterial strains

1.7. Qualitative assessment of siderophore production

1.8. Determination of the biofilm-forming ability of bacterial strains

1.9. Selection of strains exhibiting multiple plant growth–promoting mechanisms

2. Genomic analysis and taxonomic identification of the selected bacterial strains

2.1. Extraction and sequencing of the genomic DNA of bacterial strains P3.3S and P1.5S using Next Generation Sequencing (NGS) technology

2.2. De novo assembly of bacterial genomes

2.3. Taxonomic identification of the strains of interest and phylogenomic analysis

2.4. Functional annotation of bacterial genomes

3. Investigation of the antimicrobial activity of *Bacillus velezensis* P3.3S and *Bacillus safensis* P1.5S strains

3.1. Identification of biosynthetic gene clusters involved in secondary metabolites production with antimicrobial activity

3.2. Identification of extracellular lipopeptides by mass spectrometry

3.3. Evaluation of antimicrobial activity using the diffusion method

3.4. Determination of the influence of abiotic stress on the antimicrobial activity of the *Bacillus velezensis* P3.3S strain

4. Evaluation of abiotic stress effects on root colonization mechanisms in *Bacillus velezensis* P3.3S

4.1. Identification of genes involved in root colonization in the genome of *Bacillus velezensis* P3.3S

4.2. Evaluation of the chemotactic properties of *Bacillus velezensis* P3.3S

4.3. Demonstration of the motility of the *Bacillus velezensis* P3.3S strain

4.4. Quantification of biofilm formation

4.5. Analysis of the formed biofilm using scanning electron microscopy (SEM)

4.6. Visualization of the formed biofilm using confocal laser scanning microscopy (CLSM)

4.7. Evaluation of cell surface hydrophobicity through hydrocarbon adhesion

4.8. Determination of total carbohydrate content

5. Effect of abiotic factors on growth and phosphorus solubilization mechanisms in *Bacillus safensis* P1.5S

5.1. Identification of genes involved in the solubilization of phosphorus compounds and genes conferring tolerance to abiotic stress

5.2. Assessment of the effects of abiotic stress on the growth of *Bacillus safensis* P1.5S in a discontinuous asynchronous culture

5.3. Evaluation of the phosphorus solubilization potential of *Bacillus safensis* P1.5S under abiotic stress conditions

5.4. Investigation of the effects of abiotic stress on mechanisms involved in phosphorus solubilization

6. Analysis and interpretation of obtained data. Dissemination of results

6.1. Application of statistical tests for the analysis and interpretation of results

6.2. Preparation of scientific reports

6.3. Participation in national and international scientific events

6.4. Writing scientific articles for publication

6.5. Writing the doctoral thesis

PART I. CURRENT STATE OF KNOWLEDGE

CHAPTER I. THE INFLUENCE OF RHIZOSPHERIC MICROORGANISMS ON PLANTS

Food security is considered a complex concept, implying that the entire global population should always have access to sufficient, safe, and affordable food. Given that the planet faces a series of challenges such as climate change, biodiversity loss, and the increasing global population, food security is becoming increasingly fragile and difficult to achieve (FAO, 2019). Consequently, ensuring food security has become one of the key objectives of the 2030 Agenda for Sustainable Development, adopted by the United Nations (United Nations, 2015).

Plants play a fundamental role in global food security, representing the main source of human nutrition. According to studies, over 80% of the world's food requirements are provided by plants. In addition to supplying a wide range of essential food products, plants also constitute a critical resource for animal production, serving as feed for livestock raised for human consumption (FAO, 2017; Rizzo *et al*., 2021).

Soil supports plant growth by providing nutrients and water, as well as the physical support necessary for plant stability. Interactions between plants and soil occur at the root system, considered a vital part of the plant. Thus, the volume of soil surrounding plant roots forms a distinct structure with pores and interfaces, which serves as the site of numerous plant–microorganism–soil interactions (Mueller *et al*., 2024).

I.1. Plant rhizosphere

The term rhizosphere was first defined by the German researcher Lorenz Hiltner in 1904 (Berg & Smalla, 2009; Bakker *et al*., 2013). The rhizosphere represents the portion of soil surrounding the roots, which is directly influenced by the physiological and metabolic activities of plants. This zone hosts the highest density of microorganisms in the soil, including fungi, protozoa, and algae, with estimates suggesting that one gram of root may contain up to 10^{11} microbial cells (Balestrini *et al*., 2015). However, the most abundant group of microorganisms in the soil is represented by bacteria. Due to their remarkable ability to colonize roots, bacteria can significantly influence plant physiological processes as well as other categories of microorganisms (Kumar *et al*., 2020).

The rhizosphere is divided into three zones (Prashar *et al*., 2014):

- **Endorhizosphere** refers to the internal zone of the plant root, including portions of the cortex and endoderm, where microorganisms can occupy the “free space” between cells (the apoplastic space).
- **Rhizoplane** represents the immediate zone around the root, including the root epidermis and mucilage; it is the site where plant roots actively interact with the soil and microorganisms.
- **Ectorhizosphere** refers to the more extended area (a few millimeters) around the rhizosphere that encompasses the soil surrounding the roots.

I.2. Root exudates and root colonization by microorganisms

During growth and development, a wide range of organic compounds is released from the roots through processes of exudation, secretion, and deposition. Due to these three processes occurring at the root level, the rhizosphere becomes rich in nutrients that can attract beneficial microorganisms, which may enhance plant growth and development. Following photosynthesis, plants release between 11–40% of the resulting compounds as root exudates, consisting of substances with varying molecular weights. Low-molecular-weight compounds include molecules such as sugars (arabinose, deoxyribose, fructose, galactose, glucose, maltose, mannose, ribose, sucrose, and xylose), organic acids (acetic, butyric, citric, fumaric, glycolic, lactic, malic, oxalic, propionic, succinic, tartaric, and valeric), amino acids, alcohols, volatile organic compounds, and other secondary metabolites (Tate, 2021; Chen and Liu, 2024).

Research on the colonization of plant roots by bacteria has made significant progress in recent years. It has been demonstrated that this process is complex and involves several successive stages: motility, chemotaxis, and biofilm formation (Liu *et al*., 2024).

Motility. Dispersion and migration are fundamental ecological processes that allow bacteria to explore new niches, avoid unfavorable environmental conditions, and reduce competition for nutrients (Tecon and Or, 2016). Bacteria use several strategies to actively move in growth environments, with motile forces mediated by flagella and pili. Pili enable surface motility through extension, adhesion, and retraction, while flagella are rigid helical structures anchored in the cell wall that rotate to generate propulsion (Aroney *et al*., 2021). Depending on nutrient availability and the level of soil competition, bacterial motility can occur in various ways. Several types of bacterial motility have been described: swimming, swarming, twitching, gliding, and sliding (Yang and van Elsas, 2018).

Interactions in the rhizosphere are based on the recruitment of beneficial microorganisms by plants. One mechanism bacteria use to locate a potential host is **chemotaxis**, i.e., active movement

toward or away from signaling molecules (Keren *et al*., 2024). Chemotaxis is the innate ability of bacteria to detect and respond to various chemical compounds present in the plant rhizosphere, representing a crucial step in root colonization (Xu *et al*., 2024). This mechanism allows bacteria to orient themselves and move toward specific nutrient sources or chemical signals emitted by plants, thereby facilitating their interaction with the rhizosphere (Chen and Liu, 2024; Keren *et al*., 2024).

The **quorum sensing (QS) system** plays an important role in plant–bacteria and bacteria–bacteria interactions. Quorum sensing is a bacterial communication system that operates chemically, based on the production, detection, and response of cells to signaling molecules called autoinducers. This system allows groups of bacteria to synchronize their behavior in response to changes in population density and species diversity in the neighboring community (Mukherjee and Bassler, 2019).

Biofilms are assemblies of microbial cells that adhere to a biotic or abiotic surface and are embedded in an extracellular polymeric matrix. Biofilms have a highly complex, heterogeneous, and three-dimensional structure composed of microcolonies formed by microbial cells (10–25%) and the biofilm matrix, which can represent up to 90%. The structural organization of biofilms provides microbial cells with enhanced resistance under stress conditions, such as water deficit, temperature fluctuations, acidic or alkaline pH, high salinity, nutrient scarcity, antimicrobial agents, UV radiation, toxic chemicals, and contaminated environments (Mishra *et al*., 2022).

I.3. Plant growth promoting mechanisms

Within the rhizosphere microbiome, most bacteria have a positive interaction with plants and promote their growth and survival, with only a small portion considered phytopathogenic (Hakim *et al*., 2021). Bacteria that can exert beneficial effects on plant growth and development are known as „plant growth-promoting rhizobacteria" – PGPR (Singh *et al*., 2019).

PGPR act through direct and indirect mechanisms (Zaidi *et al*., 2014; Aarab *et al*., 2019). Direct mechanisms include nitrogen fixation, phosphorus and potassium solubilization, mineralization of organic phosphates, and production of phytohormones. Indirect mechanisms include the production of antimicrobial substances, polysaccharides, siderophores, and enzymes (Pandey *et al*., 2019; Wang *et al*., 2020).

I.3.1. Direct mechanisms

I.3.1.1. Solubilization of phosphorus compounds

Phosphorus solubilization, one of the most important plant growth-promoting activities, is carried out by microbial populations known as phosphorus-solubilizing microorganisms (PSM) (Zaidi *et al*., 2014; Aarab *et al*., 2019).

Solubilization of inorganic phosphorus by microorganisms mainly occurs through the production of organic acids. These acids are produced during microbial metabolism, especially through oxidative respiration or fermentation when glucose is used as a carbon source (Prabhu *et al*., 2019). The efficiency of the solubilization process depends on the type of organic acids released into the environment as well as their concentration. Moreover, the quality of the organic acids produced is more important for phosphorus solubilization than the total amount of organic acids (Scervino *et al*., 2010). Secretion of organic acids causes a decrease in soil pH, chelates cations (mainly calcium) bound to phosphate through hydroxyl and carboxyl groups, or competes with phosphate for adsorption sites, resulting in increased solubility and availability of mineral phosphates (Wei *et al*., 2018). Organic acids such as acetic, lactic, malic, oxalic, succinic, citric, and gluconic acids can form complexes with iron and aluminum in ferric and aluminum phosphates; thus, phosphorus is released into the soil and becomes available to plants (Behera *et al*., 2014).

Phosphorus-solubilizing microorganisms can dissociate inorganic phosphorus compounds but also participate in the mineralization of organic forms. Enzymes involved in the mineralization of organophosphorus compounds include nonspecific phosphatases, phytases, and lyases. Nonspecific phosphatases hydrolyze esters and anhydrides of phosphoric acid. The most studied and abundant phosphatases are phosphomonoesterases (also called phosphohydrolases or simply phosphatases). Phosphatases are classified according to soil pH into acidic and alkaline phosphatases. Acidic phosphatases predominate in acidic soils, while alkaline phosphatases are more abundant in neutral and alkaline soils (Rawat *et al*., 2020).

I.3.1.2. Production of growth regulators

Phytohormones (growth regulators) are organic substances that, at very low concentrations (<1 mM), can stimulate, inhibit, or modify plant growth and development (Gouda *et al*., 2018). Rhizobacteria are involved in stimulating plant growth and development through growth regulators such as auxins, gibberellins, cytokinins, ethylene, and abscisic acid (Singh *et al*., 2019). Indole-3-acetic acid (IAA) is the most important auxin involved in plant physiological processes. IAA participates in numerous processes, such as cell division and differentiation, photosynthesis and production of assimilatory pigments, xylem development, improvement of seed germination, induction of lateral and adventitious root formation, regulation of vegetative growth, and conferring plant resistance to stress factors (Singh *et al*., 2019). The most important amino acid secreted by root cells is tryptophan – the main molecule involved in the IAA biosynthetic pathway.

Ethylene is the simplest molecule produced by plants and is involved in a series of biological activities, inducing physiological changes at the molecular level. Its main functions include seed germination, root hair development, flower senescence, fruit ripening, and leaf abscission. The ethylene biosynthesis pathway involves the enzymatic conversion of S-adenosylmethionine to 1-aminocyclopropane-1-carboxylic acid (ACC) by ACC synthase, followed by conversion of ACC to ethylene catalyzed by ACC oxidase. At high concentrations, ethylene has a negative effect on plants. Soil bacteria can produce an enzyme, 1-aminocyclopropane-1-carboxylate deaminase, which metabolizes ACC, the direct precursor of ethylene, into α-ketobutyrate and ammonia, thereby moderating ethylene levels in plants (Kundan *et al*., 2015).

I.3.2. Indirect mechanisms

I.3.2.1. Siderophores production

Siderophore-producing microorganisms can prevent or reduce the proliferation of phytopathogenic agents by decreasing the amount of iron available in the environment. Bacterial siderophores have a very high affinity for Fe^{3+} ions in the rhizosphere of the host plant, resulting in inhibition of phytopathogen development due to unavailability of the iron required. The efficiency of biocontrol is based on the fact that bacterial siderophores bind iron more rapidly than fungal siderophores (Olanrewaju *et al*., 2017).

I.3.2.2. Antimicrobial substances and lytic enzymes production

Antimicrobial substances produced by microorganisms are secondary metabolites belonging to heterogeneous groups of low-molecular-weight organic compounds that are harmful to microbial growth or metabolic activities. They are synthesized and released into the environment in small amounts (Mercado-Blanco *et al*., 2019). In Bacillus species, lipopeptides such as iturins, surfactins, and fengycins have been studied, while in Pseudomonas species, DAPG (2,4-diacetylphloroglucinol), pyrrolnitrin, and phenazine have been investigated (Mercado-Blanco *et al*., 2019). Rizosphere bacteria synthesize a range of lytic enzymes, such as chitinases, cellulases, 1,3-glucanases, proteases, and lipases, which can cause the lysis of the cell walls of certain phytopathogenic fungi (Kundan *et al*., 2015).

CHAPTER II. THE EFFECT OF STRESS FACTORS ON PLANTS AND MICROORGANISMS

II.1. The influence of abiotic and biotic stress on plants

II.1.1. Soil pH

Soil pH represents a key abiotic factor that significantly influences the biology and physicochemical processes occurring at this level. Evidently, soil and crop productivity depend on pH. Both acidic and alkaline soils can cause a series of negative effects on plant growth and development. Thus, extreme pH variations significantly affect nutrient uptake and all other processes occurring at the soil level. Acidic soils are characterized by a deficiency of nutrients such as phosphorus, magnesium, calcium, and molybdenum, as well as by toxicity caused by aluminum, iron, and manganese (Msimbira and Smith, 2020). Among the nutrients whose availability is affected by alkaline stress are phosphorus, iron, copper, boron, and zinc (Singh *et al*., 2018).

II.1.2. Temperature

Thermal stress (high and low temperatures compared to the optimal value) represents the main abiotic factor affecting plant growth and development, inducing morphological, physiological, and biochemical changes in plants. High temperatures cause a series of negative effects, such as decreased water content, reduced stability of the cell membrane and photosynthetic rate, and hormonal changes. Moreover, thermal stress is associated with the production of reactive oxygen species (ROS), which are highly toxic and lead to the damage of proteins, lipids, carbohydrates, and DNA, ultimately resulting in cell death (Waraich *et al*., 2012). Similarly, the impact of low temperatures on plants depends on the cooling rate, exposure time, and other associated stress factors. One of the effects caused by chilling is the reduction of photosynthesis due to impaired electron transport in the thylakoids and carbon fixation, decreased content of assimilatory pigments, and reduced free phosphorus. Another negative effect is the alteration of cell membrane fluidity (Nievola *et al*., 2017).

II.1.3. Salinity

Salinity is one of the most important abiotic factors that significantly reduce agricultural crop productivity (Mishra *et al*., 2021). The accumulation of mineral salts such as NaCl, Na_2SO_4, $MgSO_4$, $NaHCO_3$, Na_2CO_3, $CaSO_4$, and $CaCO_3$ is a major characteristic of saline soils, negatively impacting plant health. Prolonged exposure to high salt concentrations (NaCl) at the root zone increases osmotic stress, generating ionic toxicity. Osmotic stress affects water uptake, seed germination, cell elongation, leaf development, lateral bud growth, lateral branching, photosynthetic rate, and the

absorption and translocation of nutrients from the roots to aerial parts, thereby negatively affecting plant growth (Mishra *et al*., 2021).

II.1.4. Drought

Water is an indispensable molecule for the growth and development of agricultural crops. The term "drought" generally implies a significant reduction of soil water content (Marchin *et al*., 2020). An increase in drought-prone areas has negatively impacted agricultural production worldwide. It is projected that by 2050, water scarcity will cause major problems for arable lands and affect two-thirds of the global population (Ahmad *et al*., 2022). Dehydration caused by water stress affects plant metabolic activities, such as respiration, chlorophyll content, sugar metabolism, photosynthesis, and nutrient translocation. Additionally, drought reduces water potential and causes stomatal closure, which impacts cell growth and elongation (Vurukonda *et al*., 2016; Lata and Gond, 2019).

II.1.5. Nutrient deficiency

Nitrogen is a macronutrient that directly influences agricultural crop productivity. It plays a key role in plant metabolism, being a constituent element of enzymes, chlorophyll, nucleic acids, proteins, and the cell wall. Consequently, nitrogen deficiency in crops significantly affects plant growth and development (Fageria and Moreira, 2011).

Phosphorus is an essential macronutrient required for plant growth and development (Behera *et al*., 2014; Awais *et al*., 2017). It is involved in regulating metabolic processes such as cell division, energy transport, macromolecular biosynthesis, photosynthesis, and respiration (Sharma *et al*., 2013; Manzoor *et al*., 2017). Phosphorus deficiency in crops negatively affects metabolic transformations, growth, and development (Lăcătușu, 2016).

Potassium is the third most important macronutrient necessary for plant growth. Potassium deficiency results in a weaker root system, slower plant growth, the formation of small seeds, and reduced quality and yield of crops (Yadav *et al*., 2017).

II.1.6. Phytopathogenic microorganisms

Plant diseases represent a serious threat to agricultural production. Annual crop losses due to plant diseases are estimated at over 30% globally and are associated with economic damages worth hundreds of billions of dollars, significantly impacting food security, regional economies, and other related socio-economic sectors. This situation is further exacerbated by post-harvest losses caused by pathogenic microorganisms. Moreover, the spread of phytopathogens is intensified by climate change, considered one of the main threats to crops worldwide (Nature Climate Change, 2021; Gai and Wang, 2024). Plants can be infected by a wide range of pathogens (bacteria, fungi, viruses, and nematodes) that differ in lifestyle, infection strategies, and target tissues affected (Singh *et al*., 2023).

II.2. The influence of abiotic stress on soil microorganisms

II.2.1. Soil pH

The most important abiotic factor that can affect soil microbiota is **pH**, which in turn is influenced by metal toxicity, soil structure and texture, water source, and the intensity of agricultural land use. Both microorganisms and plants prefer a pH between 6 and 7. Thus, soil acidity and alkalinity frequently lead to changes in the composition and metabolic processes of microbial communities (Rahman *et al*., 2021). Acidic and alkaline soils are considered to have a lower number of bacteria compared to nearly neutral soils. This difference can be explained by the fact that pH affects the solubility of organic carbon sources necessary for optimal microbial growth, while acidic pH causes the accumulation of high concentrations of aluminum, which is considered a toxic element. Similarly, bacterial abundance in alkaline soils can decrease due to the reduced solubility of certain nutrients, such as phosphorus and iron. All these effects lead to a reduction in the number of rhizospheric microorganisms and their metabolic processes (Zhou *et al*., 2024).

II.2.2. Temperature

Global warming is a large-scale phenomenon affecting the planet, with the global average temperature estimated to increase by 1.8–3.6 °C by 2100. This phenomenon influences plant development and phenological characteristics, as well as the composition, density, metabolism, and distribution of microbial communities associated with the root system. Temperature-induced stress affects microbial activity because microorganisms require an optimal temperature range for growth. It has been found that global warming influences the composition of soil microbial communities, their diversity, complexity, and the stability of interactions established between plants and microorganisms. High temperatures can also affect nutrient cycling associated with soil microorganisms, including the carbon, nitrogen, and phosphorus cycles, as well as potassium (Zhao *et al*., 2024).

II.2.3. Salinity

High concentrations of soluble salts influence microbial biomass and activity, as well as the structure of soil microbial communities. Salinity primarily reduces microbial biomass because osmotic stress leads to dehydration and cell lysis (Yan *et al*., 2015). Microorganisms adapted to osmotic stress may exhibit reduced metabolic activity because synthesizing osmolytes consumes significant amounts of energy (Ropelewska & Zapotoczny, 2017). It has been shown that some salts, such as sodium chloride, can affect soil microbial activity by reducing the total number of fungi, actinomycetes, and bacteria. Osmotic stress can be lethal for rhizospheric microorganisms. A

decrease in microbial biomass and soil respiration can lead to inhibition of decomposition and mineralization processes in the soil (Ropelewska & Zapotoczny, 2017).

II.2.4. Drought

Drought is the climatic phenomenon with the greatest impact on food security. Its severity and frequency are expected to increase considerably over the next decade. Drought has a pronounced negative effect on the soil microbiome because soil moisture and temperature are key factors determining microbial growth and activity. Moisture levels influence soil microorganisms and induce changes in microbial metabolism and structural diversity, while high temperatures negatively impact microbial biomass and abundance. The combination of water deficit and high temperature can lead to large-scale restructuring of soil communities. Increased evapotranspiration caused by drought can reduce soil water reserves, suppressing microbial activity (Rahman *et al*., 2021).

II.3. Response of stress-tolerant bacteria to abiotic factors

II.3.1. Production and accumulation of osmolytes

Osmolytes, or osmoprotective substances, represent a small group of low-molecular-weight compounds, including trehalose, glycerol, mannitol, L-proline, L-glutamate, L-glutamine, ectoine, 5-hydroxyectoine, and glycine betaine. Bacteria can accumulate osmolytes without affecting the cell's molecular processes. This accumulation also increases the free water content in the cell, allowing growth and cell division under hyperosmotic conditions. These substances enable cells to grow and divide in unfavorable environments. It has been shown that osmolytes also protect proteins, nucleic acids, and other vital molecular mechanisms. Accumulation of osmolytes can occur either through cellular transport or biosynthesis. These compounds are also used in various metabolic pathways within the cell and as carbon sources (Gregory & Boyd, 2021).

II.3.2. Production and accumulation of antioxidants

To overcome abiotic stress, plants secrete antioxidant enzymes. The most important antioxidant enzymes produced by plants include catalase (CAT), superoxide dismutase (SOD), glutathione reductase (GR), glutathione S-transferase (GST), glutathione peroxidase (GPX), peroxidase (POD), ascorbate peroxidase (APX), polyphenol oxidase (PPO), and phenylalanine ammonia-lyase (PAL) (Yasmeen *et al*., 2020).

II.3.3. Production of extracellular polymeric substances

Extracellular polymeric substances (EPS) are biodegradable high-molecular-weight polymers synthesized by numerous bacteria, algae, and plants. EPSs consist of a complex mixture of

biomolecules forming a 3D matrix that includes polysaccharides, sugars, structural proteins, enzymes, lipids, glycoproteins, extracellular DNA, and some humic substances (Bhagat *et al*., 2021). EPSs play a central role in maintaining water potential, aggregating soil particles, ensuring obligatory contact between plant roots and rhizobacteria, and protecting roots from abiotic stress factors and phytopathogens (Naseem *et al*., 2018).

CHAPTER III. BIOTECHNOLOGICAL IMPORTANCE OF PLANT GROWTH-PROMOTING BACTERIA

III.1. Biofertilizers

The prolonged use of chemical fertilizers has increased agricultural productivity; however, it has also led to negative effects such as environmental pollution and imbalances within agricultural ecosystems. Repeated application of chemical fertilizers causes harmful environmental impacts, including contamination of groundwater and surface waters with phosphates and nitrates, decreased oxygen levels in aquatic systems, and fish mortality due to water eutrophication. Additionally, soil pH is negatively affected, leading to increased pest populations and ecosystem disturbances (Rana *et al*., 2020).

Improving soil fertility is one of the most common strategies used to increase crop production. Maintaining high levels of available nitrogen and phosphorus—the two most limiting nutrients in soil-represents a major challenge for farmers (Nautiyal *et al*., 2000; Pang *et al*., 2018).

In the long term, phosphorus sources used in the production of chemical fertilizers can have a negative impact on soil microbiota, causing substantial reductions in microbial respiration and metabolic activity (Sharma *et al*., 2013). Moreover, the efficiency of applied P fertilizers rarely exceeds 30%, due to fixation as iron/aluminum phosphate in acidic soils or calcium phosphate in neutral to alkaline soils. It has been suggested that the total phosphorus present in agricultural soils would be sufficient to support maximum crop yields worldwide if it were made available to plants (Sharma *et al*., 2013).

Phosphorus is considered a finite resource, and due to the high rate of utilization, it is estimated that high-quality rock phosphate reserves used in fertilizer production will be depleted within this century. Subsequently, lower-quality rock phosphate will be used in fertilizer manufacturing, increasing production costs. Awareness of these issues has led to the identification of a feasible strategy to improve crop yields in phosphorus-deficient soils. The use of biofertilizers possessing phosphate-solubilizing activity in agricultural soils represents an eco-friendly alternative that can enhance crop productivity (Sharma *et al*., 2013; Zhang *et al*., 2017).

It is well established that soil microorganisms play a key role in the mobilization and transformation of phosphorus, making them suitable as biofertilizers for increasing agricultural productivity (Richardson & Simpson, 2011; Lavania & Nautiyal, 2013; Wei *et al*., 2018). Biofertilizers are products containing living microorganisms, which can be applied to seeds, seedlings, or directly to soil, colonizing the rhizosphere and ultimately stimulating plant growth. Seed treatment is considered the most commonly used method for biofertilizer application due to the small quantity of product required for inoculation and the simplicity of the procedure (Mącik *et al*., 2020).

III.2. Biopesticides

Plant diseases cause significant losses in fruit and vegetable production, both during cultivation and throughout handling, transport, and storage. To maintain crop yields, plants are often treated with synthetic pesticides, which, despite their effectiveness in controlling diseases caused by phytopathogens, do not represent a sustainable solution due to their high costs and impacts on human health and the environment (Lengai & Muthomi, 2018). It is well known that these compounds can cause cancer and fetal disorders and persist in the environment for long periods due to their non-degradable nature (Kumar *et al*., 2021). Moreover, repeated use of the same pesticide can induce resistance in pathogenic microorganisms.

For these reasons, current research focuses on developing efficient and eco-friendly technologies aimed at reducing or eliminating the use of synthetic fungicides in agriculture. One promising alternative involves the use of microbial agents in biocontrol (Morales-Cedeño *et al*., 2021). Microbial agents, or antagonists, function to mitigate the harmful effects of phytopathogenic agents.

The suppression of phytopathogens by microorganisms can occur in two main periods: pre-harvest and post-harvest. Generally, the pre-harvest period includes prophylactic activities aimed at eliminating potential pathogens. Once fruits and vegetables are harvested, they must be transported and stored, during which they remain susceptible to pathogen attack. Economic losses during both periods can vary, sometimes exceeding 50% of the total yield (Morales-Cedeño *et al*., 2021).

PART II. PERSONAL CONTRIBUTIONS

CHAPTER I. SCREENING OF BACTERIAL STRAINS WITH POTENTIAL TO STIMULATE PLANT GROWTH

I.1. Research materials and methods

I.1.1. Isolation of phosphate-solubilizing microorganisms

Bacteria capable of solubilizing inorganic phosphate were isolated from three soil samples collected from maize (*Zea mays* L.) fields:

a. Sample 1: soil from a maize field with yellowing plants.
b. Sample 2: soil from a maize field with normal, healthy plants.
c. Sample 3: soil from a maize field located in a saline-affected area.

Additionally, another source of isolation was a sample of influent collected from a municipal wastewater treatment plant.

Bacterial colonies exhibiting a clear halo around them were considered to have potential for solubilizing tricalcium phosphate in the culture medium.

I.1.2. Assessment of tricalcium phosphate solubilization potential

The ability of bacterial strains to solubilize tricalcium phosphate was initially evaluated qualitatively using the PVK agar medium (Sarikhani *et al*., 2019). Based on the solubilization index obtained, the strains were classified according to their potential. Subsequently, a quantitative determination was performed by cultivating the strains in PVK broth and measuring the released phosphate using the ammonium phosphomolybdate method (Artenie *et al*., 2008; Khadraji *et al*., 2017).

I.1.3. Determination of indole-3-acetic acid (IAA) production

Bacterial capacity to synthesize indole-3-acetic acid (IAA) from tryptophan present in the culture medium was assessed using the Salkowski reagent. This reagent is a mixture of 0.5 M ferric chloride ($FeCl_3$) and 35% perchloric acid ($HClO_4$), which reacts with IAA to form a pink tris(indole-3-acetate) iron (III) complex. The intensity of the pink color was measured spectrophotometrically at 530 nm (Gang *et al*., 2019).

I.1.4. Detection of 1-aminocyclopropane-1-carboxylate deaminase (ACCD) activity

The enzyme ACC deaminase (ACCD) reduces ethylene levels in plants, a hormone associated with stress. ACCD catalyzes the conversion of 1-aminocyclopropane-1-carboxylic acid (ACC), the

immediate ethylene precursor, into α-ketobutyrate ($C_4H_6O_3$) and ammonia (NH_3), promoting optimal plant growth (Shahid *et al*., 2023).

I.1.5. Evaluation of antifungal activity of bacterial strains

The antifungal potential of bacterial strains was assessed by co-culturing them with target fungal strains on the same medium. Inhibition zones around bacterial inocula indicated the production and diffusion of substances with antifungal activity.

I.1.6. Assessment of siderophore production

The CAS (chrome azurol S) assay was used to detect siderophore production. In this medium, the CAS-Fe^{3+}-HDTMA complex serves as an indicator. When strong iron chelators produced by bacteria remove iron from the complex, a color change occurs in the surrounding medium, indicating siderophore production (Louden *et al*., 2011).

I.1.7. Biofilm biomass determination using crystal violet staining

Biofilm formation by bacterial strains was assessed in 96-well microplates. The biofilm biomass was quantified by staining with 1% crystal violet, followed by solubilization with 30% acetic acid. The intensity of the resulting color is directly proportional to the biofilm biomass (Ansari & Ahmad, 2018).

I.2. Results and discussions

Analyzing the results obtained in this chapter, it was observed that bacterial strains isolated both from soils cultivated with maize and from the wastewater sample exhibited multiple plant growth-promoting mechanisms (Tables I.1 and I.2). Among the soil isolates, strains P1S and P3.3S demonstrated all the tested properties. In contrast, strain P1.5S was capable of solubilizing tricalcium phosphate, producing IAA, ACCD, and siderophores, as well as forming biofilm, but it was unable to suppress the growth of the tested phytopathogenic fungi. Strain P2.1S exhibited only tricalcium phosphate solubilization and IAA production, while the other mechanisms were not detected using the applied methods (Table I.1).

Table I.1. Plant growth-promoting mechanisms identified in bacterial strains isolated from soils cultivated with maize

Bacterial strains	P solubilization	IAA	ACCD	Siderophores	Antifungal activity	Biofilm
P1S	++	++	+	+	+	++

Bacterial strains	P solubilization	IAA	ACCD	Siderophores	Antifungal activity	Biofilm
P1.1S	+++	-	-	+	-	-
P1.5S	+++	++	+	++	-	+++
P2S	+++	+	+	-	-	+++
P2.1S	+++	+++	-	-	-	-
P2.2S	+++	+++	++	-	-	+++
P3.1S	+++	+	+	-	-	+
P3.2S	++	+++	++	-	-	+++
P3.3S	+	+	++	+++	+++	+++
P3.4S	+++	+	++	-	-	+++

(+++) – high potential; (++) – medium potential; (+) – low potential; (-) – absent potential

In the case of isolates from wastewater, it was observed that antifungal activity was not detected for any bacterial strain. However, most strains exhibited mechanisms such as tricalcium phosphate solubilization, IAA production, ACCD activity, siderophore production, and biofilm formation (Table I.2).

Table I.2. Plant growth-promoting mechanisms identified in bacterial strains isolated from wastewater

Bacterial strains	P solubilization	IAA	ACCD	Siderophores	Antifungal activity	Biofilm
D1	++	+	++	++	-	+
D2	+++	++	+	++	-	+
D3	+	+	+	+++	-	+
D4	++	++	++	-	-	+
D5	+	++	+	+	-	++
D6	+++	+	++	+	-	+++
D7	+	+	+++	-	-	+
D8	++	+	+	+	-	+++
D9	++	++	+	-	-	+++
D10	+	+	+	+++	-	+++
D11	+	+	+	-	-	++
D12	+++	+	+	-	-	+
D13	++	+	+	+++	-	++
D14	+++	+	+	-	-	++
D15	+++	+++	++	-	-	+++
D16	+	+	+	-	-	+++
D17	+	+	+	+++	-	++

Bacterial strains	P solubilization	IAA	ACCD	Siderophores	Antifungal activity	Biofilm
D18	+	+	+++	-	-	+++
D19	+++	+	+++	-	-	+
D20	++	+	+++	+	-	++
D21	+++	++	+++	-	-	+

(+++) – high potential; (++) – medium potential; (+) – low potential; (-) – absent potential

The objective of this chapter was to select strains that could later be used to investigate the influence of stress factors on tricalcium phosphate solubilization, antimicrobial activity, and biofilm formation. Bacterial strains isolated from wastewater were not selected for experiments regarding phosphorus solubilization under stress conditions, as a decrease in the amount of solubilized phosphorus was observed when these strains were tested at certain time intervals. Furthermore, experiments determining solubilized P for strains P3.4S and P2.1S showed that the potential for tricalcium phosphate solubilization significantly decreases over time. Considering these findings, strain P1.5S was selected to evaluate the effects of abiotic stress on tricalcium phosphate solubilization potential, as it is among the three strains isolated from maize-cultivated soils that solubilized the highest amounts of phosphorus under optimal growth conditions, maintaining a relatively stable solubilization potential over time. On the other hand, the only strain that showed promising antifungal activity against the three tested species was P3.3S, which also forms the largest amount of biofilm. Therefore, strain P3.3S was selected for studying antimicrobial activity and biofilm formation under stress conditions.

CHAPTER II. GENOMIC ANALYSIS OF THE SELECTED BACTERIAL STRAINS

II.1. Research materials and methods

II.1.1. Isolation and sequencing of genomic DNA

The genomic DNA was isolated following the manufacturer's instructions for the DNeasy UltraClean Microbial Kit (Qiagen). The genomic DNA obtained from the two selected bacterial strains was sequenced using the Illumina NovaSeq 6000 platform (Macrogen Europe BV, Amsterdam, Netherlands).

II.1.3. De novo assembly of bacterial genomes

The genomes of the two bacterial strains were assembled using two programs: SPAdes 3.15.4 (Bankevich *et al*., 2012) for the assembly of the P3.3S strain genome, and Unicycler 0.4.9 (Wick *et al*., 2017) for the P1.5S strain.

II.1.4. Taxonomic identification of selected strains

The data obtained from genome assembly were uploaded to the TYGS (Type (Strain) Genome Server) (Meier-Kolthoff & Göker, 2019) for taxonomic identification and phylogenomic analysis.

II.1.5. Functional annotation of bacterial genomes

Functional annotation of the two genomes was performed using RAST (Rapid Annotation using Subsystem Technology) (Aziz *et al*., 2008) and NCBI PGAP (Prokaryotic Genome Annotation Pipeline) (Tatusova *et al*., 2016).

II.2. Results and discussions

II.2.1. Genomic characterization of bacterial strains P3.3S and P1.5S

The assembled genomes have been submitted to NCBI GenBank and are accessible under the accession numbers JARXQM000000000 (strain P3.3S) and JARZFW000000000 (strain P1.5S).

The draft genome of strain P3.3S has a length of 3,860,972 bp (base pairs) and consists of 22 contigs, represented by a single replicon with an N50 (the shortest contig length at which 50% of the genome is contained in contigs of that length or longer) of 479,779 bp and a G+C content of 46.65%.

In contrast, the draft genome of strain P1.5S is smaller (3,667,318 bp) and contains only 13 contigs. Its replicon has an N50 of 975,127 bp and a G+C content of 41.5%.

For both bacterial strains, the programs used did not detect the presence of plasmids.

II.2.2. Taxonomic classification and phylogenomic analysis of the bacterial strains

The phylogenetic tree (Figure II.1) consisted of two separate clades sharing a common ancestor. The first clade was further divided into two branches: one branch included only the strain *Bacillus nakamurai* NRRL B-41091, while the second branch was itself split into two sub-branches. One sub-branch contained a single strain, *Bacillus amyloliquefaciens* DSM 7, whereas the other sub-branch was divided into two parts: one part included the strains *B. siamensis* KCTC 13613 and *B. vanillea* XY18, and the other part comprised the strain P3.3S, which clustered with *Bacillus amyloliquefaciens* subsp. *plantarum* FZB62, *Bacillus oryzicola* KACC 18228T, *Bacillus velezensis* NRRL B-41580, and *Bacillus methylotrophicus* KACC 13105.

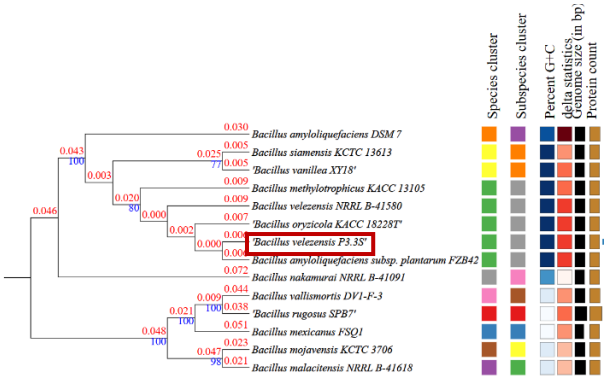

Figure II.1. Phylogenetic tree based on the whole genome of the *Bacillus velezensis* P3.3S strain. The tree was constructed using FastME 2.1.6.1, which employs phylogenetic distances between genome sequences. Branch lengths (red numbers) are scaled according to the D5 formula of Genome BLAST Distance Phylogeny (GBDP). Numbers shown in blue indicate pseudo-bootstrap GBDP values >60% from 100 replicates, with an average branch support of 71.5%.

As observed in Figure II.1, the bacterial strain P3.3S shares the same species-level cluster (species cluster) with *Bacillus amyloliquefaciens* subsp. *plantarum* FZB62, *Bacillus oryzicola* KACC 18228T, *Bacillus velezensis* NRRL B-41580, and *Bacillus methylotrophicus* KACC 13105, indicating a high degree of genomic similarity among these strains. This similarity is supported by the digital DNA-DNA hybridization (dDDH) values obtained for the aforementioned strains in comparison with P3.3S: 90.5%, 89.2%, 85.7%, and 84.9%, respectively (Table II.1). These results allowed the identification of strain P3.3S as belonging to the species *Bacillus velezensis*.

Table II.1. dDDH comparisons between the genome of *Bacillus velezensis* P3.3S and the genomes of type strains selected by TYGS. Shown are the dDDH values, their confidence intervals for formula d4, and the differences in G+C content.

Type bacterial strains	dDDH (%) (d4)	C.I (%) (d4)	G+C differences (%)
Bacillus amyloliquefaciens subsp. *plantarum* FZB42	90,5	(88,2 - 92,3)	0,17
Bacillus oryzicola KACC 18228T	89,2	(86,8 - 91,2)	0,21
Bacillus velezensis NRRL B-41580	85,7	(83,0 - 88,0)	0,33
Bacillus methylotrophicus KACC 13105	84,9	(82,2 - 87,3)	0,22
Bacillus siamensis KCTC 13613	56,9	(54,1 - 59,6)	0,31
Bacillus vanillea XY18	56,8	(54,0 - 59,5)	0,33

Type bacterial strains	dDDH (%) (d4)	C.I (%) (d4)	G+C differences (%)
Bacillus amyloliquefaciens DSM 7	55,8	(53,1 - 58,5)	0,57
Bacillus nakamurai NRRL B-41091	30,9	(28,5 - 33,4)	1,39
Bacillus malacitensis NRRL B-41618	20,4	(18,1 - 22,8)	3,13
Bacillus rugosus SPB7	20,3	(18,1 - 22,7)	3,53
Bacillus mexicanus FSQ1	20,2	(18,0 - 22,6)	3,69
Bacillus vallismortis DV1-F-3	20,2	(18,0 - 22,6)	2,89
Bacillus mojavensis KCTC 3706	20,2	(18,0 - 22,6)	2,98

dDDH = *digital DNA-DNA hybridization* calculated using d4 formula (Meier-Kolthoff and Göker, 2019).

CI = confidence intervals

For strain P1.5S, based on the TYGS analysis, a phylogenetic tree was constructed, divided into two clades sharing a common ancestor (Figure II.2). The first clade was split into two branches. One branch contains strain P1.5S together with *Bacillus safensis* subsp. *osmophilus* CECT 9344T, *B. safensis* FO-36b, *B. australimaris* NH7I_1, and two strains of *B. pumilus* (ATCC 7061 and NCTC 10337); the other branch consists solely of *B. zhangzhouensis* MCCC 1A08372. The second clade was further divided into two branches. The first branch was split into two sub-branches: the first includes *B. invictae* DSM 26896 and *B. aerius* 24K, while the second contains *B. cellulasensis* NCIM 5461 and *B. altitudinis* DSM 21631. The last branch was represented by *B. xiamenensis* HYC-10 (Figure II.2).

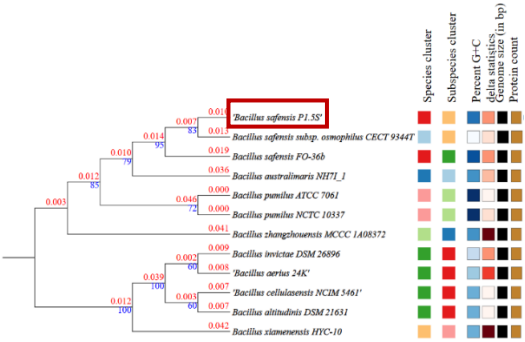

Figure II.2. Phylogenetic tree based on the whole genome of *Bacillus safensis* strain P1.5S. The tree was constructed using FastME 2.1.6.1, which relies on phylogenetic distances between genome sequences. Branch lengths (red numbers) are scaled according to the D5 formula of Genome BLAST Distance Phylogeny. Blue numbers represent GBDP pseudo-bootstrap support values > 60% from 100 replicates, with an average branch support of 81.6%.

The P1.5S strain was clustered together with *B. safensis* FO-36b and *B. safensis* subsp. *osmophilus* CECT 9344T in a single branch. TYGS analysis also indicated a dDDH value of 80.6% in comparison with *Bacillus safensis* subsp. *osmophilus* CECT 9344T, and 70.7% in comparison with *Bacillus safensis* FO-36b (Table II.2). Based on these results, we concluded that strain P1.5S belongs to the species *Bacillus safensis*.

Table II.2. dDDH comparisons between the genome of *Bacillus safensis* P1.5S and the genomes of type strains selected by TYGS. The table shows the dDDH values, their confidence intervals for formula d4, and the differences in G+C content.

Type bacterial strains	dDDH (%) (d4)	C.I (%) (d4)	G+C differences (%)
Bacillus safensis subsp. *osmophilus* CECT 9344T	80,6	(77,7 - 83,2)	0,6
Bacillus safensis FO-36b	70,7	(67,7 - 73,6)	0,11
Bacillus australimaris NH7I 1	52,3	(49,7 - 55,0)	0,15
Bacillus pumilus NCTC 10337	45	(42,4 - 47,6)	0,22
Bacillus pumilus ATCC 7061	44,9	(42,4 - 47,5)	0,17
Bacillus zhangzhouensis MCCC 1A08372	42,1	(39,6 - 44,7)	0,11
Bacillus xiamenensis HYC-10	37,5	(35,1 - 40)	0,2
Bacillus invictae DSM 26896	36,6	(34,2 - 39,2)	0,39
Bacillus aerius 24K	36,6	(34,1 - 39,1)	0,28
Bacillus altitudinis DSM 21631	36,6	(34,1 - 39,1)	0,23
Bacillus cellulasensis NCIM 5461	36,5	(34,0 - 39,0)	0,17

dDDH = *digital DNA-DNA hybridization* calculated using d4 formula (Meier-Kolthoff and Göker, 2019).
C.I = confidence intervals.

II.2.3. Functional annotation of the strain genomes P3.3S and P1.5S

According to the functional annotation performed by RAST, it was observed that the draft genome of the strain *B. velezensis* P3.3S is divided into 321 subsystems, contains 3949 coding sequences and 54 RNA genes. In turn, the strain *B. safensis* P1.5S presents 320 subsystems, 3831 coding sequences and 46 RNA genes. The RAST analysis assigned a theoretical function to only 30% of the genes present in the draft genome. In the case of both strains, the RAST analysis indicated that most of the genes are involved in the metabolism and transport of amino acids, carbohydrates and proteins, the production of cofactors, vitamins, prosthetic groups and pigments. In addition, genes involved in sporulation and dormancy were identified (Figure II.3).

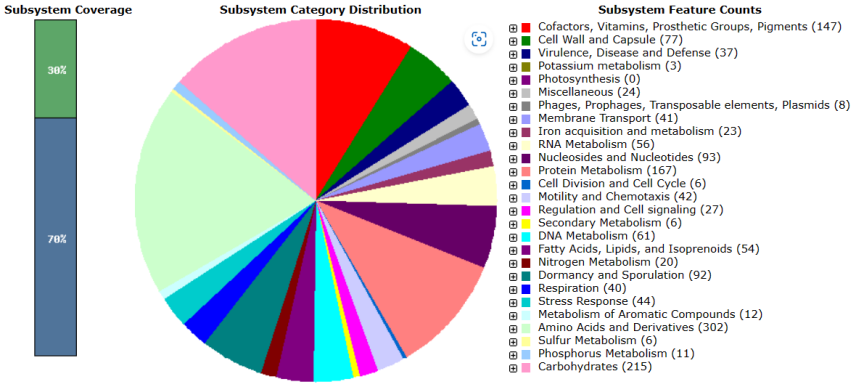

A

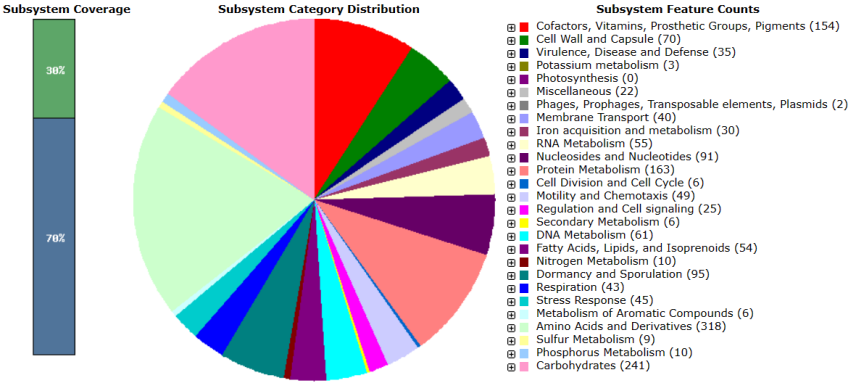

B

Figure II.3. Distribution of functional subsystems in the genomes of the bacterial strains *Bacillus velezensis* P3.3S (A) and *Bacillus safensis* P1.5S (B), according to the annotation performed with RAST. The colors in the chart indicate the major subsystems, as mentioned in the legend. The circular chart was generated and visualized with SEED Viewer.

According to the functional annotation of the *B. velezensis* P3.3S genome performed with the NCBI Prokaryotic Genome Annotation Pipeline (PGAP), a total of 3,826 genes were predicted, including tRNAs = 46, ncRNAs = 5, and 5 rRNA operon sets (1 set – 5S rRNA, 2 sets – 16S rRNA, 2 sets – 23S rRNA). In addition, the genome contains 66 pseudogenes. On the other hand, the genome of *B. safensis* P1.5S comprises a total of 3,748 genes, tRNAs = 44, ncRNAs = 5, and only two rRNA operon sets (16S and 23S).

CHAPTER III. ANTIMICROBIAL ACTIVITY OF *BACILLUS VELEZENSIS* P3.3S AND *BACILLUS SAFENSIS* P1.5S

III.1. Research materials and methods

III.1.1. Identification of gene clusters responsible for the biosynthesis of secondary metabolites with potential antimicrobial activity

To identify the presence of genes responsible for the synthesis of secondary metabolites with potential antimicrobial activity in the genomes of the selected strains, the web server antiSMASH 7.0 (Blin *et al*., 2023) was used. antiSMASH (antibiotics Secondary Metabolite Analysis Shell) enables rapid identification, annotation, and genome-wide analysis of gene clusters involved in secondary metabolite biosynthesis.

III.1.2. Identification of extracellular lipopeptides by mass spectrometry

MALDI-TOF mass spectrometry (Matrix-Assisted Laser Desorption/Ionization – Time of Flight Mass Spectrometry) is suitable for identifying biomolecules such as peptides, lipids, carbohydrates, and other organic macromolecules. Mass spectra were analyzed using FlexAnalysis software (version 4.1, Bruker), and molecules with antimicrobial activity were identified by comparing the molecular weights obtained in the mass spectra with those available in the NORINE database (Flissi *et al*., 2019).

III.1.3. Evaluation of antimicrobial activity using diffusion methods

Antibacterial activity was assessed by measuring the inhibition zones of *Agrobacterium tumefaciens* GV220 growth around wells containing supernatant and filtrate obtained after centrifugation of the bacterial cultures of interest (P3.3S and P1.5S). Antifungal activity was determined by calculating the percentage inhibition of fungal mycelium growth (*Rhizoctonia solani, Fusarium oxysporum, Sclerotinia sclerotiorum, Verticillium dahliae*). To evaluate the effect of pH, salinity, and drought on the antimicrobial activity of the *B. velezensis* P3.3S strain, it was cultivated in YEB medium with: pH 5, 6, 8, 9; NaCl concentrations: 2.5, 10, 15, 20, 25, 30, 35, and 40 g/L; PEG8000 concentrations: 8, 12, 15, 17.7, and 20%; the control consisted of YEB medium at pH 7 without NaCl or PEG8000.

III.2. Results and discussions

III.2.1. The genomes of the *Bacillus safensis* P1.5S and *Bacillus velezensis* P3.3S strains contain genes involved in the biosynthesis of secondary metabolites with antimicrobial activity

The antiSMASH analysis allowed the identification of 11 gene clusters in the genome of *Bacillus velezensis* P3.3S involved in the production of secondary metabolites. Among these 11 clusters, 5 are located in node 1, while nodes 2, 4, 5, 6, 11, and 12 each contain a single cluster. Out of these, only seven clusters showed significant similarity to those previously reported in the MIBiG (Minimum Information about a Biosynthetic Gene cluster) database – Figure III.1. For six clusters, a 100% similarity with the database was obtained, linking them to the biosynthesis of bacillaene (region 1.1), fengycin (region 1.2), difficidin (region 1.5), bacilysin (region 2.1), macrolactin H (region 6.1), and bacillibactin (12.1). Another identified molecule was surfactin (region 4.1), with a similarity of 95%. Clusters 1.3, 1.4, 6.1, and 11.1 could not be identified, as they showed no similarity with any compounds available in the database (Figure III.1).

Initially, the automated antiSMASH analysis did not identify the biosynthetic gene cluster responsible for iturin production in the genome of *B. velezensis* P3.3S. This is unusual because the gene cluster for iturins is typically found in species such as *B. amyloliquefaciens*, *B. siamensis*, and *B. velezensis*. A manual verification of the results revealed that the biosynthetic gene cluster in region 1.2, associated with fengycin production, actually contains two adjacent gene groups: one responsible for fengycin or plipastatin biosynthesis, and another containing genes related to the synthesis of compounds from the iturin family (bacillomycin D, mycosubtilin, paenilarvin, or other iturin-like substances). The similarity with the database was 100% for genes involved in fengycin, plipastatin, bacillomycin, mycosubtilin, and paenilarvin biosynthesis, and 88% for genes involved in iturin production (Figure III.1).

A similar situation was observed for region 12.1. At first glance, the gene cluster in this region is assigned to bacillibactin production, but a more detailed analysis showed that this region actually contains two gene groups: one involved in bacillibactin or paenibactin production, and another cluster responsible for the synthesis of amylocyclicin. In this case as well, the similarity percentage was 100%.

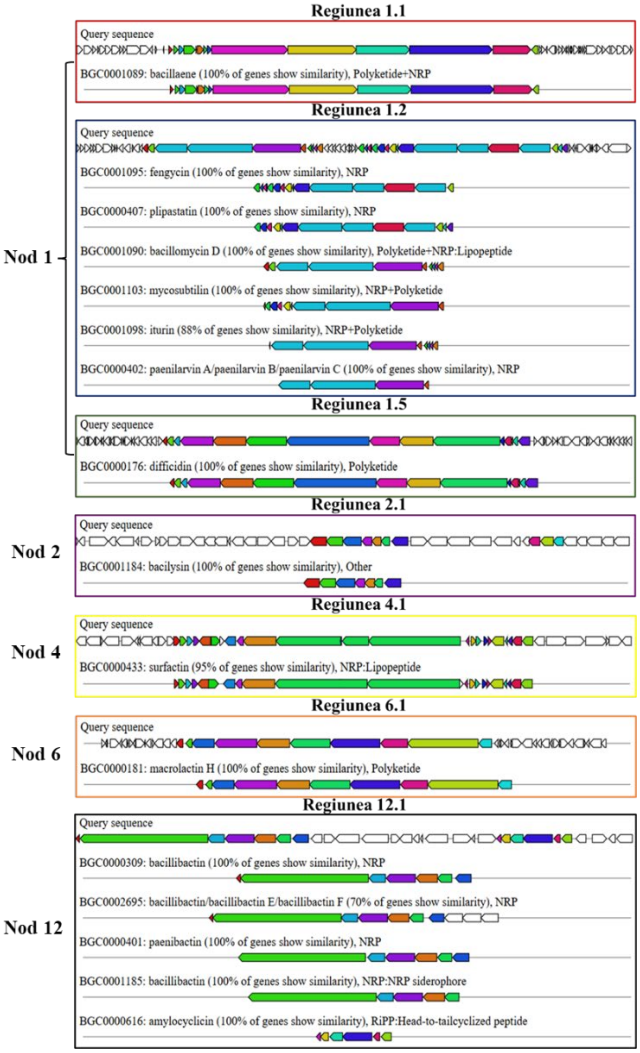

Figure III.1. Biosynthetic gene clusters involved in the production of secondary metabolites with antimicrobial activity identified in the genome of *Bacillus velezensis* P3.3S using the antiSMASH webserver. Regions 1.1, 1.2, and 1.5 were identified in node 1, region 2.1 in node 2, region 4.1 in node 4, region 6.1 in node 6, and region 12.1 in node 12. Within each box corresponding to the mentioned regions, the biosynthetic gene clusters identified in the genome of *B. velezensis* P3.3S (query sequence) and the secondary metabolites from the Minimum Information about a Biosynthetic Gene cluster (MIBiG) database that showed similarity with the queried sequence are presented.

Regarding the *Bacillus safensis* P1.5S strain, the antiSMASH analysis allowed the identification of 12 gene clusters involved in the biosynthesis of secondary metabolites (Figure III.2). Among the identified clusters, 4 are present in node 1, 2 in node 2, 2 in node 3, 2 in node 5, and one each in nodes 6 and 10. Four clusters show no similarity with the database. Unlike the clusters previously identified in the P3.3S strain, these showed low similarity percentages with the database and are associated with the synthesis of fengycin (53%, region 1.1), botromicin A2 (6%, region 1.4), bacilysin (85%, region 2.1), bacillibactin (80%, region 2.2), schizokinen (60%, region 3.1), and surfactin (39%, region 6.1). Two of the identified gene clusters were associated with the production of lichenysin (50% – region 5.2, and 14% – region 10.1) – Figure III.2.

As also observed in the genome of the *B. velezensis* P3.3S strain, the gene cluster involved in the production of the siderophore bacillibactin identified in the genome of *B. safensis* P1.5S is also responsible for the synthesis of paenibactin, with a similarity percentage of 100% (Figure III.2).

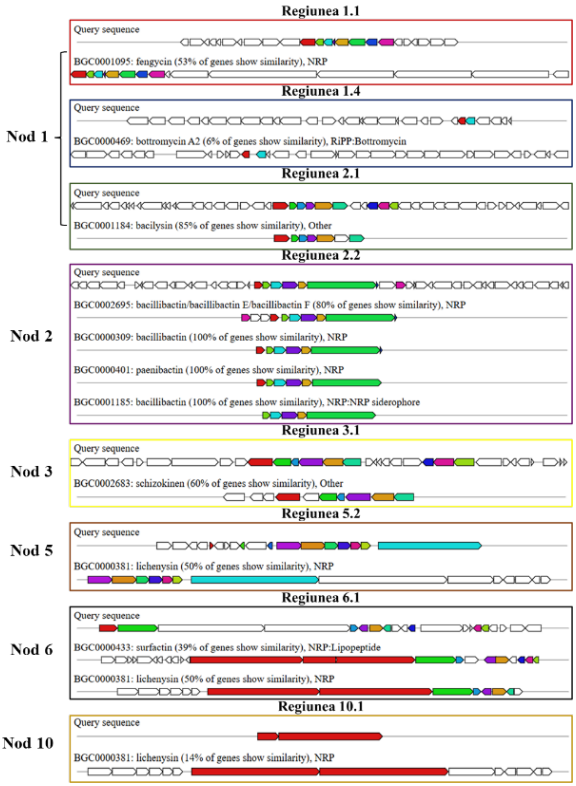

Figure III.2. Biosynthetic gene clusters involved in the production of antimicrobial secondary metabolites identified in the genome of *Bacillus safensis* P1.5S using the antiSMASH webserver. Regions 1.1 and 1.4

were identified in node 1, regions 2.1 and 2.2 in node 2, region 3.1 in node 3, region 5.2 in node 5, region 6.1 in node 6, and region 10.1 in node 10. In each box corresponding to the mentioned regions, the biosynthetic gene clusters identified in the genome of *B. safensis* P1.5S (query sequence) are shown, along with the secondary metabolites from the Minimum Information about a Biosynthetic Gene cluster (MIBiG) database that showed similarity with the queried sequence.

III.2.2. The selected bacterial strains produce antimicrobial lipopeptides

MALDI-TOF analysis of the culture supernatant of the strain *Bacillus velezensis* P3.3S indicated the presence of molecules with different molecular weights belonging to the three classes of lipopeptides: surfactin, iturin, and fengycin (Figure III.3). Thus, secondary metabolites belonging to the surfactin class were identified at 1043 Da (surfactin C13+K+/[Val7]surfactin C14+K+/[Ala4]surfactin C15+K+, surfactin C15+K+), 1074 Da (surfactin C15+K+/[Ile7]surfactin C15+K+) (Figure III.3.A). From the iturin class, strain P3.3S produces bacillomycin L+K+/bacillomycin D5+K+ (1059 Da) and iturin C1 with molecular weights ranging between 1098 Da (iturin C1 C18+K+/H+) and 1150 Da (iturin C1 C19+K+/H+) (Figure III.3.A). Compounds with a molecular weight of 1087 Da were identified either as [Gln1] surfactin C16+K+ or as bacillomycin L4+K+. Most spectra corresponded to biomolecules from the fengycin class. Their molecular weight ranged from 1463 to 1543 Da. Among the compounds produced by strain P3.3S are fengycin A C14–C17+K+/H+ and fengycin B C15–C17+K+/H+ (Figure III.3.B). In addition to the three classes of lipopeptides, MALDI-TOF analysis also revealed the presence of bacillibactin+K+ (921 Da) – Figure III.3.A.

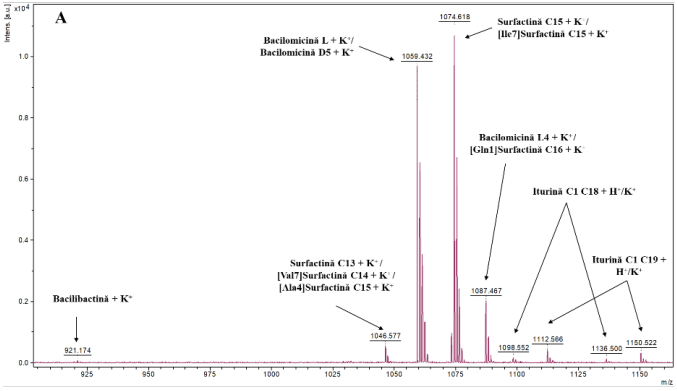

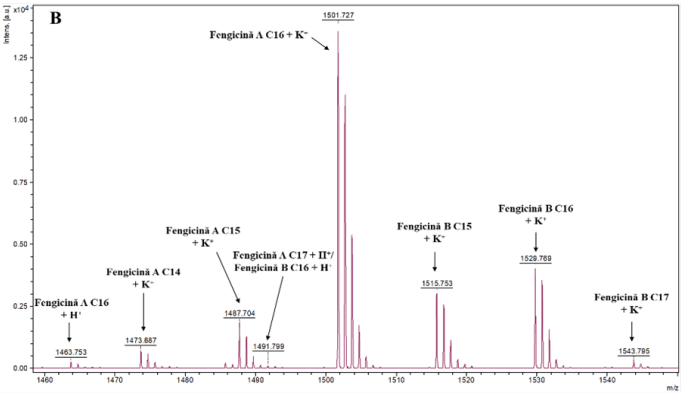

Figure III.3. Molecules with antimicrobial activity identified in the culture supernatant of *Bacillus velezensis* P3.3S by MALDI-TOF mass spectrometry after 72 hours of cultivation in Landy medium. A – spectra corresponding to the production of bacillibactin, bacillomycin, iturin, and surfactin; B – spectra corresponding to the production of fengycin.

Following the analysis of the spectra obtained by MALDI-TOF, it was observed that the *B. safensis* P1.5S strain synthesizes fewer molecules with antimicrobial activity compared to the *B. velezensis* P3.3S strain. The presence of a single class of lipopeptides and the siderophore bacillibactin+K+ (921 Da) was noted. Three molecular weights corresponding to different surfactin isomers were identified: 1060 – surfactin C14+K+/[Val7] surfactin C15+K+/[Ile7] surfactin C14+K+; 1074 – surfactin C15+K+/[Ile7] surfactin C15+K+; 1088 – surfactin C16+K+/[Val7] surfactin C17+K+ (Figure III.4).

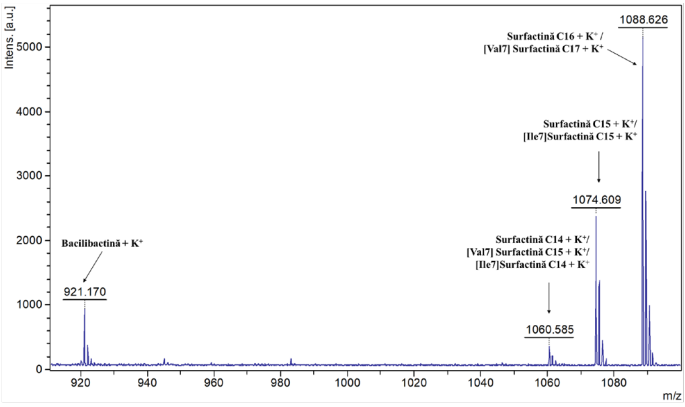

Figure III.4. Antimicrobial molecules identified in the culture supernatant of *Bacillus safensis* P1.5S by MALDI-TOF mass spectrometry after 72 h of cultivation in Landy medium.

III.2.3. The *Bacillus velezensis* P3.3S strain exhibits antimicrobial activity against phytopathogenic microorganisms

MALDI-TOF analysis revealed the production of molecules known to have antimicrobial activity, which is why we aimed to perform tests to confirm the antimicrobial potential of the *Bacillus velezensis* P3.3S and *Bacillus safensis* P1.5S strains against five phytopathogenic agents: the bacterial strain *Agrobacterium tumefaciens* GV220, and the fungi *Rhizoctonia solani*, *Fusarium oxysporum*, *Sclerotinia sclerotiorum*, and *Verticillium dahliae*.

III.2.3.1. Antibacterial Activity

The results obtained from the direct antagonism test highlighted that the *Bacillus velezensis* P3.3S strain exhibits antibacterial activity against the tested phytopathogenic bacterium. Notably, the culture filtrate inhibited the growth of *A. tumefaciens* GV220, demonstrating the production and release of molecules with antibacterial activity into the culture medium (Figure III.5). In contrast, *Bacillus safensis* P1.5S did not produce inhibition zones against the growth of *A. tumefaciens* GV220 (Figure III.5).

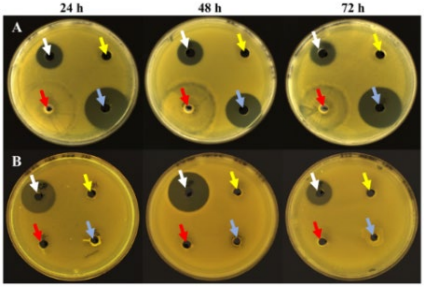

Figure III.5. Antibacterial activity of *Bacillus velezensis* P3.3S (A) and *Bacillus safensis* P1.5S (B) against Agrobacterium tumefaciens GV220. In the wells of the plates, the following were added: kanamycin 100 µg/mL – white arrows; sterile YEB medium – yellow arrows; supernatant – red arrows; filtrate – blue arrows.

Regarding the antibacterial activity of the *Bacillus velezensis* P3.3S strain, the diameters of the inhibition zones against *Agrobacterium tumefaciens* GV220 varied depending on the incubation time of the tested bacterial culture as well as the sample used (supernatant or filtrate). For the supernatant obtained after centrifugation of the *B. velezensis* P3.3S culture, inhibition zones ranged between 34 and 37 mm. Regarding the culture filtrate, a lower inhibition of the phytopathogenic bacterium was observed, with diameters between 22 and 27.5 mm, the maximum value being measured at 24 hours of incubation of the P3.3S bacterial culture. It is noteworthy that the culture filtrate of *B. velezensis* P3.3S was more effective in inhibiting the growth of the tested *A. tumefaciens* strain compared to kanamycin (100 µg/mL) at 24, 48, and 72 hours (Table III.1).

Table III.1. Diameters of inhibition zones of Agrobacterium tumefaciens GV220 growth in the presence of *Bacillus velezensis* P3.3S. Values represent the mean of two determinations ± standard error of the mean.

Variants tested	Diameter of the inhibition zone (mm)		
	24 h	48 h	72 h
Kanamycin (100 µg/mL)	16 ± 0	16 ± 1	15,5 ± 0,5
Supernatant	35 ± 0	37 ± 2	34 ± 4
Filtrate	27,5 ± 0,5	22 ± 2	26 ± 2

III.2.3.2. Antifungal activity

Following the direct antagonism test, it was found that the strain *Bacillus velezensis* P3.3S exhibits antifungal activity against all four tested phytopathogenic species: *Rhizoctonia solani*, *Sclerotinia sclerotiorum*, *Fusarium oxysporum*, and *Verticillium dahliae* (Figure III.6). Notably, for *Sclerotinia sclerotiorum* and *Fusarium oxysporum*, there is no direct contact between the fungal mycelium and the bacterial strain, suggesting the secretion and diffusion into the medium of substances with antifungal activity such as surfactin, iturin, bacillomycin, fengycin, and bacillibactin, as confirmed by mass spectrometry.

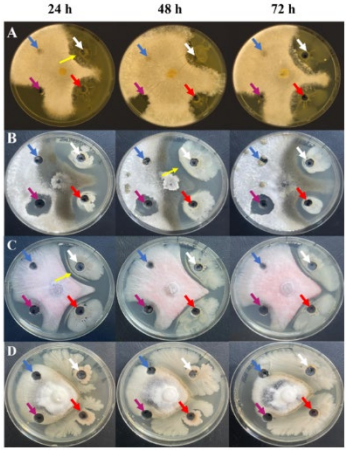

Figure III.6. Antifungal activity of the *Bacillus velezensis* P3.3S strain against *Rhizoctonia solani* (A), *Sclerotinia sclerotiorum* (B), *Fusarium oxysporum* (C), and *Verticillium dahliae* (D). The wells in the plate contained: sterile YEB medium (negative control) – blue arrows; bacterial culture – white arrows; supernatant – purple arrows; filtrate – red arrows. Yellow arrows indicate the zones of fungal mycelium growth inhibition.

The *Bacillus velezensis* P3.3S strain inhibited the mycelial growth of all four tested phytopathogenic species, with the highest inhibition percentages observed for the bacterial culture, followed by the supernatant and then the filtrate. For the *B. velezensis* P3.3S culture, inhibition

percentages ranged from 58.03% (*V. dahliae*, 72 h) to 70.7% (*Rhizoctonia solani*, 24 h) – Figure III.7. Regarding the supernatant, the strongest activity was observed against *Sclerotinia sclerotiorum* at 48 h, with an inhibition percentage of 65% (Figure III.7-B).

The bacterial culture filtrate also exhibited significant activity against three of the tested fungal species, with *S. sclerotiorum* mycelial growth being the most affected, showing inhibition percentages between 57.27% and 61.45% (Figure III.7-B). On the other hand, the lowest activity was observed for *Verticillium dahliae*, with inhibition percentages ranging from 5.95% to 10.35% (Figure III.7-D). This difference in antifungal activity may be related to the prolonged incubation of *V. dahliae* with the filtrate (20 days), during which the secondary metabolites present in the bacterial filtrate could have lost stability and, consequently, activity.

For all tested fungal species, except *Sclerotinia sclerotiorum* (Figure III.7-B), significant differences were observed between the antifungal activity of the three types of samples analyzed: bacterial culture, supernatant, and filtrate. For *Fusarium oxysporum* and *Verticillium dahliae*, the inhibition percentage associated with the filtrate was significantly lower compared to the values obtained for the bacterial culture and supernatant at all time intervals investigated (Figure III.7-C, D). In the case of *Rhizoctonia solani*, the antifungal activity of the filtrate decreased considerably at 24 h (55.05%) and 48 h (50%) compared to the bacterial culture, while at 72 h, the filtrate efficiency (39.66%) was also lower than that of the supernatant.

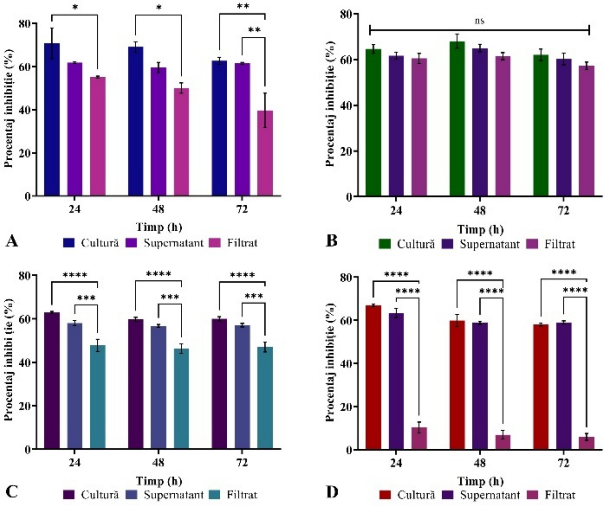

Figure III.7. Percentages of inhibition of mycelial growth of *Rhizoctonia solani* (A), *Sclerotinia sclerotiorum* (B), *Fusarium oxysporum* (C), and *Verticillium dahliae* (D) recorded for the *Bacillus velezensis* P3.3S strain.
The values shown represent the mean of two experimental determinations. The bars represent the standard error

of the mean. Asterisks indicate significant differences (* = $p < 0.05$, ** = $p < 0.01$, *** = $p < 0.001$; **** = $p < 0.0001$); ns – no significant differences.

Following the evaluation of the antifungal activity of the *B. safensis* P1.5S strain against the four tested phytopathogenic species (*Rhizoctonia solani, Sclerotinia sclerotiorum, Fusarium oxysporum,* and *Verticillium dahliae*), it was found that this strain inhibits only the mycelial growth of *Rhizoctonia solani* at 24 h, with an inhibition percentage of 50.58%. For the other tested species, the fungal mycelium developed across the entire surface of the PDA medium, regardless of the incubation time or the tested variant (Figure III.8).

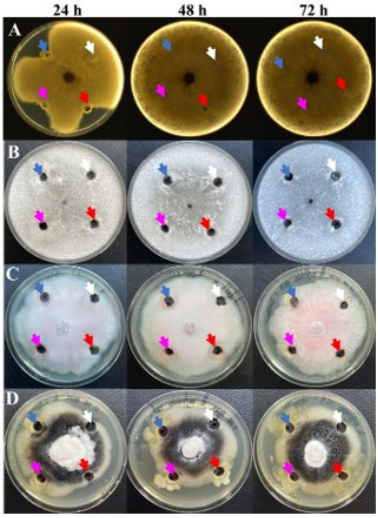

Figure III.8. Results of the direct antagonism tests between *Bacillus safensis* P1.5S and *Rhizoctonia solani* (A), *Sclerotinia sclerotiorum* (B), *Fusarium oxysporum* (C), and *Verticillium dahliae* (D). In the wells prepared on the plate, the following were added: sterile YEB medium (negative control) – blue arrows; bacterial culture – white arrows; supernatant – purple arrows; filtrate – red arrows.

III.2.4. Influence of abiotic stress factors on the antimicrobial activity of *Bacillus velezensis* P3.3S

The antimicrobial activity of the *B. velezensis* P3.3S strain was evaluated under abiotic stress conditions (pH, salinity – NaCl, and drought – PEG8000). The test microorganisms used were *A. tumefaciens* GV220 and *S. sclerotiorum*, which showed the best growth inhibition results. Measurements were taken after 24 hours of cultivating the *B. velezensis* P3.3S strain in YEB medium modified to simulate the aforementioned abiotic stress conditions. The filtrate of each bacterial culture was used as the test sample.

The effect of sodium chloride on the antibacterial activity of the *B. velezensis* P3.3S strain varied depending on the concentration used. Supplementing the YEB medium with 2.5, 10, 15, and 20 g/L NaCl stimulated the inhibition of *A. tumefaciens* GV220 growth, with inhibition zone diameters ranging from 23.18 to 27.5 mm, compared to the control (YEB medium without NaCl) where the diameter was 21.66 mm (Figure III.9-A). On the other hand, at higher NaCl concentrations (25, 30, and 35 g/L), the antibacterial activity of the P3.3S strain against *A. tumefaciens* GV220 was negatively affected, with inhibition zone diameters decreasing as the NaCl concentration increased, until at 40 g/L NaCl no growth inhibition was observed (Figure III.9-A).

The concentrations of PEG8000 used to simulate water stress did not affect the antibacterial activity of the *Bacillus velezensis* P3.3S strain against *A. tumefaciens* GV220. The bacterial culture filtrates produced inhibition zones ranging from 21.93 to 24.75 mm, compared to the control where the diameter was 21.66 mm. Moreover, the filtrate obtained after cultivating the strain in YEB medium containing 8, 12, and 15% PEG8000 showed significantly higher activity than the control ($p < 0.05$), indicating a stimulation of secondary metabolite production with antibacterial activity.

The antibacterial activity of *B. velezensis* P3.3S against *A. tumefaciens* GV220 also varied depending on the initial pH of the YEB medium used for cultivation. Maximum activity was observed at pH 6, with an inhibition zone diameter of 23.75 mm, statistically significant compared to the control (21.66 mm) and to the other tested pH values. The efficiency of inhibiting *A. tumefaciens* GV220 growth decreased as the initial pH of the medium increased, with the smallest inhibition zones (13 mm) recorded after cultivation in YEB medium with a strongly alkaline initial pH of 9 (Figure III.9-C).

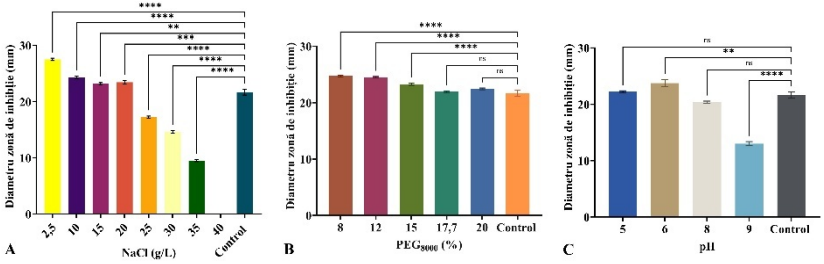

Figure III.9. Influence of NaCl (A), PEG8000 (B), and medium pH (C) concentrations on the antibacterial activity of the *Bacillus velezensis* P3.3S strain against *Agrobacterium tumefaciens* GV220. The values shown represent the mean of two experimental determinations. Error bars indicate the standard error of the mean. Asterisks denote significant differences (** = $p < 0.01$, *** = $p < 0.001$, **** = $p < 0.0001$); ns – no significant differences.

The antifungal activity of *Bacillus velezensis* P3.3S against the phytopathogenic species *Sclerotinia sclerotiorum* varied depending on the tested conditions. Filtrates obtained after cultivating

the strain in YEB medium supplemented with 2.5, 10, and 15 g/L NaCl showed slightly higher antifungal activity, with inhibition percentages ranging from 48.90 to 52.56%. However, these values were not significantly different from the control, represented by the filtrate of *B. velezensis* P3.3S grown in YEB without NaCl (46.50%) (Figure III.10-A). Starting from 20 g/L NaCl, antifungal activity decreased as the NaCl concentration increased, from 36.96% to 25.26% (recorded at 35 g/L NaCl). Similarly to antibacterial activity, a concentration of 40 g/L NaCl did not inhibit the *S. sclerotiorum* mycelium (Figure III.10-A).

Regarding the effect of PEG8000 concentrations on antifungal activity, inhibition percentages of *S. sclerotiorum* mycelium ranged from 51.28 to 54.88%, compared to the control (46.82%), represented by the filtrate obtained from the strain grown in YEB without PEG8000 (Figure III.10-B). Antifungal activity was significantly higher in filtrates obtained from cultures grown in YEB supplemented with 8% and 12% PEG8000 compared to the control.

The antifungal activity of *B. velezensis* P3.3S was also maintained when cultivated in YEB with different pH values, except at strongly alkaline pH 9, which did not inhibit the fungal mycelium. Filtrates obtained from cultivation at pH 5, 6, and 8 inhibited the development of *S. sclerotiorum*, with the maximum inhibition percentage observed at pH 6 (54.09%) (Figure III.10-C). Statistical analysis showed no significant differences between the inhibition zones obtained at pH 5, 6, or 8 and the control, represented by the filtrate of *B. velezensis* P3.3S grown in YEB with neutral initial pH (7).

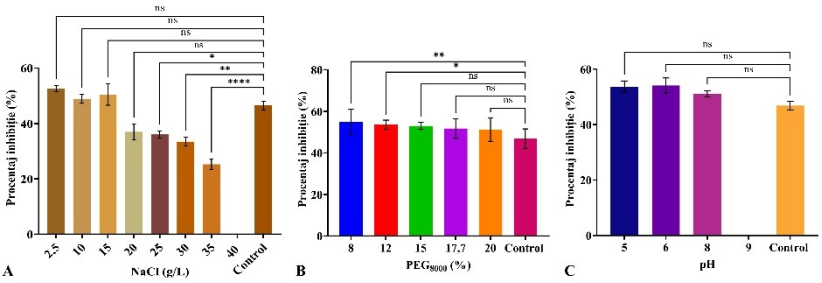

Figure III.10. Influence of NaCl (A), PEG8000 (B) concentrations, and medium pH (C) on the antifungal activity of *B. velezensis* P3.3S against *Sclerotinia sclerotiorum*. The values shown represent the mean of two experimental determinations. Error bars represent the standard error of the mean. Asterisks indicate significant differences (* = $p < 0.05$, ** = $p < 0.01$; **** = $p < 0.0001$); ns – no significant differences.

CHAPTER IV. EFFECT OF ABIOTIC STRESS FACTORS ON THE MECHANISMS INVOLVED IN ROOT COLONIZATION BY *BACILLUS VELEZENSIS* P3.3S

IV.1. Research materials and methods

The mechanisms involved in root colonization (motility, biofilm formation) were evaluated under abiotic stress conditions represented by pH (5, 6, 7, 8, 9), salinity (2.5, 10, 15, 20, 25, 30, 35, 40 g/L NaCl), and drought (8, 12, 15, 17.7, 20% PEG8000).

IV.1.1. Identification of genes involved in root colonization

The BLAST algorithm was used to identify genes of interest in the genome of the *B. velezensis* P3.3S strain. Genes with an identity greater than 30% and a coverage percentage above 70% were considered positive hits.

IV.1.2. Evaluation of chemotactic properties

The ability of the bacteria to move toward specific compounds was highlighted in vitro using a chemotactic system consisting of three elements: the chemotactic agent (organic acids and sugars), a sterile 200 µL pipette tip (used as a chamber), and a 1 mL syringe with a needle (Sharma *et al*., 2020).

IV.1.3. Highlighting the motility of bacterial cells

The swimming and swarming motility of the *Bacillus velezensis* P3.3S strain, in the presence of the investigated stress factors, was evaluated macroscopically by assessing the area colonized on semi-solid media.

IV.1.4. Quantification of microbial biofilm by crystal violet staining

Biofilm quantification was performed by staining with a 1% crystal violet solution. Subsequently, the bound dye was solubilized with 30% acetic acid, and the color intensity measured spectrophotometrically was directly proportional to the number of cells in the biofilm (Ansari and Ahmad, 2018).

IV.1.5. Analysis of biofilms using scanning electron microscopy

Scanning electron microscopy (SEM) allows the analysis of the surface of biofilms produced by bacteria and can highlight the presence of extracellular polymeric substances secreted by the cells.

IV.1.6. Visualization of the biofilm using laser scanning confocal microscopy

To highlight the influence of abiotic factors (pH, salinity, and drought) on biofilm formation by the *B. velezensis* P3.3S strain, photographs were taken in different microscopic fields to visualize the biofilm's architecture and thickness.

IV.1.7. Assessment of cell surface hydrophobicity through adherence to hydrocarbons

To determine the percentage of hydrophobicity, the following formula was used (Ansari and Ahmad, 2019):

$$\text{Percentage of hydrophobicity} = \frac{\text{OD400 initiall} - \text{OD400 final}}{\text{OD400 initial}} \times 100$$

IV.1.8. Determination of total carbohydrate content

For the determination of total carbohydrate content, the phenol–sulfuric acid method described by Nielsen (2017) was used. The compounds formed by the action of sulfuric acid condense with phenol to produce stable yellow-golden compounds, which can be measured spectrophotometrically (Nielsen, 2017).

IV.2. Results and discussions

IV.2.1. The genome of the *B. velezensis* P3.3S strain contains genes responsible for mechanisms involved in colonization

The *B. velezensis* P3.3S strain has 19 genes involved in chemotaxis and motility, with an identity percentage ranging from 49.10% to 94.17%. These include: *cheA, cheB, cheC, cheR, cheV, cheY, cheW, tlpAB, mcpABC, motAB, swrABCD*. Additionally, four genes involved in the quorum sensing signaling system were identified in the *B. velezensis* P3.3S genome: *luxS, comA, comP, comQ*. Moreover, BLAST analysis identified several genes involved in biofilm formation (*spo0A, tapA, sipW, tasA, sinR, sinI, ylbF, ymcA, yuaB*), production of extracellular polymeric substances (*epsC-O*), γ-polyglutamic acid (*pgsA-C*), surfactin (*srfAA, srfAB, srfAC, srfAD*), as well as genes regulating these processes.

IV.2.2. The *B. velezensis* P3.3S strain exhibits chemotactic properties

The capillary chemotaxis assay revealed that the *Bacillus velezensis* P3.3S strain was attracted to all tested compounds; however, the relative chemotactic response (RCR) varied depending on each substance used. RCR was highest following exposure of bacterial cells to glucose (30.66), followed by fumaric acid (28.33), citric acid (27.66), maltose (26.33), malic acid (25.66), fructose (21.33), and succinic acid (3.66) – Figure IV.1.

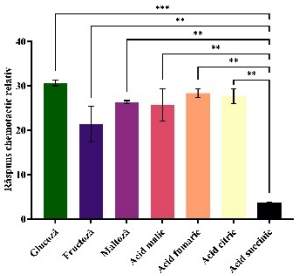

Figure IV.1. Relative chemotactic response of the *Bacillus velezensis* P3.3S strain following exposure of bacterial cells to different organic compounds. The relative chemotactic response represents the ratio between colony-forming units developed after exposure to the chemoattractant and those of the control (sterile distilled water). The values shown are the average of two experimental determinations. Error bars represent the standard error of the mean. Asterisks indicate significant differences (** = $p < 0.01$; *** = $p < 0.001$).

IV.2.3. Motility of *Bacillus velezensis* P3.3S under stress conditions

When cultivated on semisolid NB medium, the *Bacillus velezensis* P3.3S strain exhibited both swimming and swarming motility. Moreover, the strain was able to spread across the entire surface of the medium regardless of the type of stress factor tested. The only observable differences, for both swimming and swarming motility, were related to the macroscopic appearance of the colony on the medium surface.

For swimming motility, a uniform movement of bacterial cells was observed when grown on medium at pH 7 and 9. At pH 5 and 6, the colonized surface showed a non-uniform aspect, while at pH 8, intersecting lines forming branches could be observed (Figure IV.2-A).

Regarding swarming motility, a compact colony appearance was noted, determined by the uniform movement of bacterial cells from the point of inoculation on NB medium at pH 7 (control) – Figure IV.2-B. At pH 5, a more pronounced zone around the central colony was observed, with cell density decreasing toward the periphery. When cultivated at pH 6, the colonies displayed a markedly different appearance compared to other pH values, forming two concentric rings on the medium surface, with the central ring being more pronounced. At pH 8 and 9, cells moved symmetrically and uniformly, with this type of motility characterized by group movement of cells (Figure IV.2-B).

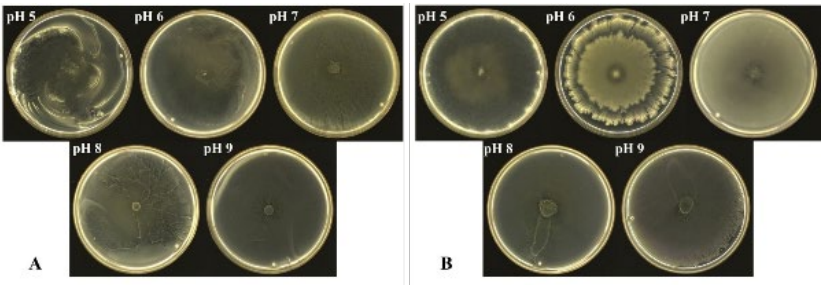

Figure IV.2. Influence of pH on the swimming (A) and swarming (B) motility of *Bacillus velezensis* P3.3S. Cultivation was performed on NB medium with 0.3% and 0.5% agar for 24 hours. The control corresponded to NB culture medium at pH 7**.**

Cultivation of the bacterial strain *B. velezensis* P3.3S on semisolid NB medium showed that both types of motility are not affected by the NaCl concentrations used, with bacterial cells being able to move across the entire surface of the medium even at a concentration of 40 g/L (Figure IV.3). Moreover, the appearance of the colonies formed on the medium surface was not as variable as observed in the investigations regarding the effect of pH.

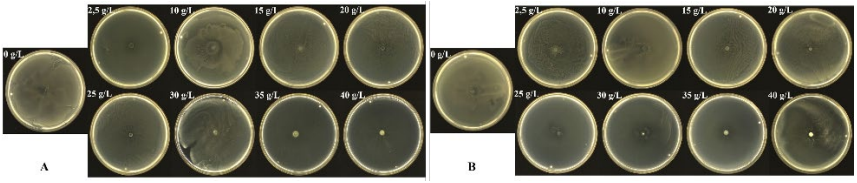

Figure IV.3. Influence of NaCl concentrations (g/L) on the swimming (A) and swarming (B) motility of the *Bacillus velezensis* P3.3S strain. Cultivation was carried out on NB medium with 0.3% and 0.5% agar for 24 h. The values in the figure represent NaCl concentrations. The control consisted of NB medium with 0 g/L NaCl.

Following the cultivation of the *B. velezensis* P3.3S strain on NB medium supplemented with different concentrations of PEG8000, it was observed that the bacterial cells were able to move across the surface of the medium even when the water content of the medium was lower, noting that at 20% PEG concentration the colony exhibited an uneven appearance, with cells moving in a disorganized manner on both NB medium with 0.3% and 0.5% agar (Figure IV.4).

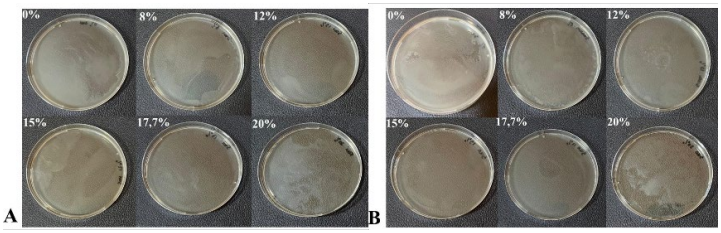

Figure IV.4. Influence of PEG8000 concentrations on the swimming (A) and swarming (B) motility of the *Bacillus velezensis* P3.3S strain. Cultivation was performed on NB medium with 0.3% and 0.5% agar for 24 hours. The percentages shown in the figure represent the concentrations of PEG8000 with which the NB medium was supplemented. The control was represented by NB medium with 0% PEG8000.

IV.2.4. The *Bacillus velezensis* P3.3S strain can form biofilms under abiotic stress conditions

The biofilm biomass varied when cultivated at different pH values (Figure IV.5). The highest amount of biofilm was observed at pH 6, with a maximum absorbance value of 9.62, which was statistically significant compared to the absorbance value measured for the control (pH 7 = 8.72). In contrast to the control (pH 7), acidic pH (5) led to a decrease in the amount of bacterial biofilm formed (7.70). Similar results were obtained when the *B. velezensis* P3.3S strain was cultivated in LB medium at pH 8 and 9, showing a reduction in biofilm quantity (pH 8 = 2.08; pH 9 = 1.96), which was statistically significant when the strain was exposed to alkaline pH (Figure IV.5).

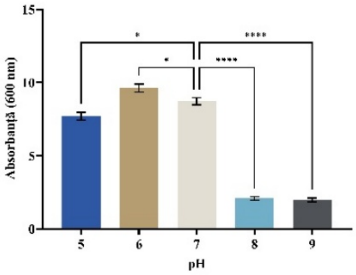

Figure IV.5. Influence of pH on the ability of the *Bacillus velezensis* P3.3S strain to form biofilm in LB medium over 48 h. The control was represented by the strain inoculated in LB medium at pH 7. The values shown represent the mean of two experimental determinations. Error bars indicate the standard error of the mean. Asterisks denote significant differences (* = $p < 0.05$, **** = $p < 0.0001$).

Increasing NaCl concentrations in the culture medium resulted in a significant decrease in the amount of biofilm formed by the *Bacillus velezensis* P3.3S strain (Figure IV.6). The maximum biomass was recorded at 10 g/L NaCl (8.72), which was considered the experimental control. Supplementing the LB medium with 2.5 g/L NaCl led to a significant reduction in biofilm formation

(7.61) compared to the control. Furthermore, absorbance values decreased as the NaCl concentrations increased. Absorbance readings ranged from 0.904 (40 g/L NaCl) to 2.06 (15 g/L NaCl) and were statistically different from the control (8.72), according to the Tukey test.

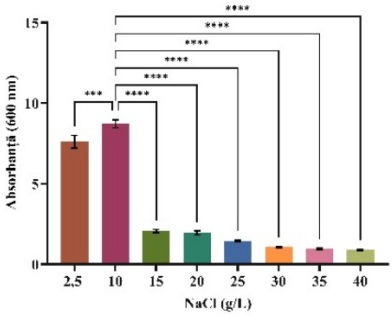

Figure IV.6. Influence of salinity on the ability of *Bacillus velezensis* P3.3S to form biofilm in LB medium over 48 h. The control was represented by the strain inoculated in LB medium supplemented with 10 g/L NaCl. The values shown represent the mean of two experimental determinations. Error bars represent the standard error of the mean. Asterisks indicate significant differences (** = $p < 0.01$, **** = $p < 0.0001$).

The results obtained from cultivating the *Bacillus velezensis* P3.3S strain in LB medium supplemented with different concentrations of PEG8000, used to simulate water stress, showed a different behavior of the strain compared to that observed when testing the influence of pH and salinity. While previously the strain's potential to form biofilm decreased with increasing pH and NaCl concentrations, in this case, the biofilm biomass increased significantly as the PEG8000 concentration in the medium increased up to 15%, remaining approximately constant at 17.7% and 20% PEG8000, compared to the control (0% PEG8000). The absorbance values measured ranged from 8.63 (0% PEG) to 32.11, recorded at 15% PEG.

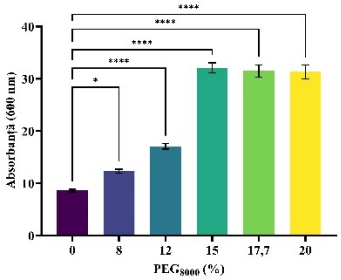

Figure IV.7. Influence of PEG8000 concentrations on the ability of *Bacillus velezensis* P3.3S to form biofilm in LB medium over 48 h. The control was represented by LB medium without PEG8000 supplementation. The

values shown represent the mean of two experimental determinations. Error bars represent the standard error of the mean. Asterisks indicate significant differences (* = $p < 0.05$, **** = $p < 0.0001$).

IV.2.5. Architecture of biofilms formed by *Bacillus velezensis* P3.3S under stress conditions

Images obtained using SEM revealed that the morphology of the biofilm formed by *Bacillus velezensis* P3.3S varies depending on the stress factor investigated (Figure IV.8). The biofilm formed at pH 7 (control) has a tree-bark-like appearance, with visible channels (marked with yellow arrows) on its surface (Figure IV.8-A). A similar morphology to the biofilm formed at pH 7 can also be observed at 20 g/L NaCl (Figure IV.8-M).

Compared to the control, a distinct morphology was observed for biofilms formed at 2.5 g/L NaCl and 8% PEG8000, where bacterial cells are organized in chains that intertwine into a complex network, giving the biofilm a spongy appearance (Figures IV.8-J, K, L, P).

The biofilm formed at 15% PEG8000 differs from the control and from the other biofilms analyzed. At this concentration, the biofilm consists of small bacterial cells arranged in thick chains (Figure IV.8-S), embedded in a matrix likely serving to protect the cells from osmotic stress (Fessia *et al*., 2022).

Biofilms formed by *B. velezensis* P3.3S under the tested stress conditions exhibit a complex structure, with bacterial cells closely connected, most likely due to the production of extracellular polymeric substances (EPS) (marked with white arrows) (Bridier *et al*., 2013). These EPS give the biofilms a gelatinous appearance, observed prior to dehydration for SEM visualization. The EPS forming the biofilm matrix were most clearly visible in the biofilm formed at pH 9 (Figures IV.8-G, H). This mucoid matrix prevented direct visualization of the embedded cells, with only their shapes being discernible; however, a small region confirmed the presence of bacteria beneath the matrix (Figure IV.8-I).

The presence of EPS was also noted in the other biofilms analyzed. In the control and at 20 g/L NaCl, EPS exhibited a spider-web-like network (marked with white arrows), enveloping the bacterial cells (Figure IV.8-C). Following exposure to different PEG8000 concentrations (8% and 15%), bacterial cells were entirely embedded in an amorphous substance. Careful examination of the biofilm surface revealed clusters of granules (marked with blue arrows) (Figures IV.8-Q, T).

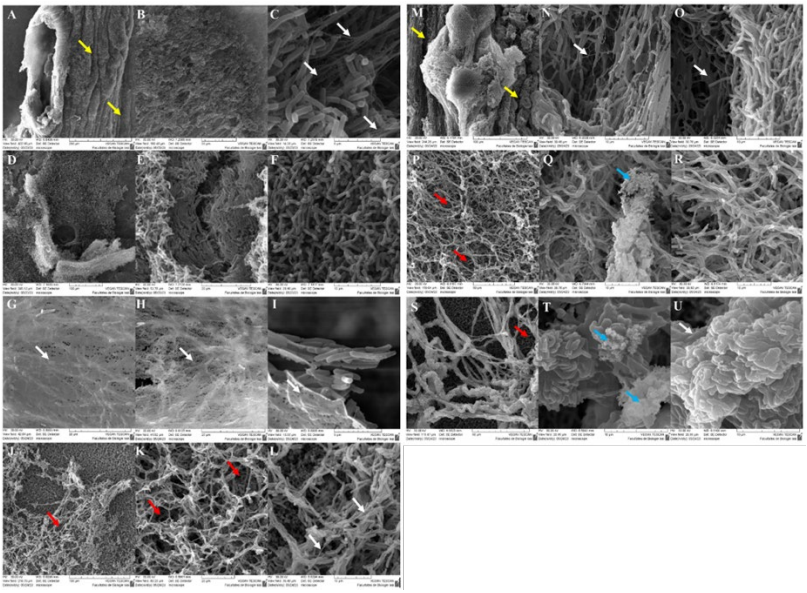

Figure IV.8. Scanning electron microscopy images showing the morphology of biofilms formed under abiotic stress by *Bacillus velezensis* P3.3S: Control (A, B, C), pH 5 (D, E, F), pH 9 (G, H, I), 2.5 g/L NaCl (J, K, L), 20 g/L NaCl (M, N, O), 8% PEG8000 (P, Q, R), 15% PEG8000 (S, T, U). The control corresponds to the biofilm formed in LB medium with pH 7, 10 g/L NaCl, and 0% PEG8000. Biofilms were formed on 0.45 µm pore filters by incubating for 48 hours in LB medium at 30 °C. White arrows indicate the presence of extracellular polymeric substances (EPS). Yellow arrows indicate the presence of channels. Blue arrows point to EPS granules, and red arrows indicate internal spaces within the biofilm.

The tested strain formed a strong, compact, and very dense biofilm on the surface of the glass slide under cultivation in LB medium with pH 7 and 10 g/L NaCl (considered the experimental control) – Figure IV.9. The results showed that the biofilms formed by this strain exhibited different conformations depending on the tested condition. Specifically, the characteristic chaining of bacterial cells within the biofilm was observed when cultivated in medium at pH 5 (Figure IV.9-A, pH 5). At both 20 g/L and 40 g/L NaCl, gaps were observed within the biofilm, most likely due to biofilm formation around salt crystals that formed on the surface of the glass slide and were visible under bright-field illumination (Figure IV.9-A, 20 g/L and 40 g/L NaCl).

Analysis of the 2D images at 8% PEG8000 showed that the biofilm formed was very thin, with only a few cells attached to the glass surface (Figure IV.9-A, 8% PEG8000). However, 3D projections of the images revealed that the biofilm was compact and very dense (Figure IV.9-B, 8% PEG8000). Column C in Figure IV.9 shows the layers of cells within the biofilm, indicating variations in

thickness depending on the tested condition. The thickness of the biofilm can also be visualized in Column D of Figure IV.9, which represents the fluorescence intensity of the formed biofilm. Fluorescence intensity depends on the number of cell layers; therefore, biofilms with more cell layers exhibit higher fluorescence intensity. Additionally, Column D highlights the irregular morphology of biofilms formed under stress conditions, as reported in the literature (Mishra *et al*., 2022).

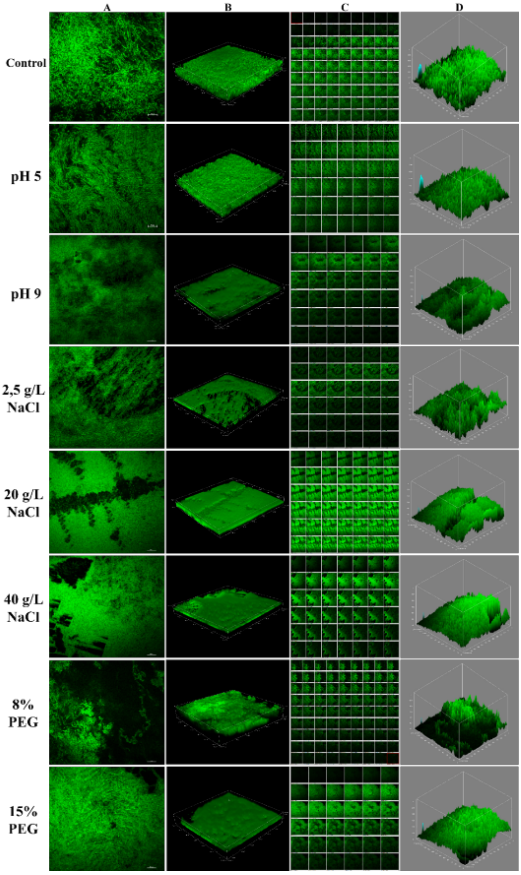

Figure IV.9. Architecture of the mature biofilm formed by the *B. velezensis* P3.3S strain under different stress conditions, visualized by laser scanning confocal microscopy: A – 2D images; B – 3D projection of the images; C – layers of bacterial cells within the biofilm; D – graphical representation of fluorescence intensity from the 2D images, analyzed using ImageJ. Biofilms were formed on glass slides by incubating for 48 hours at 30 °C. Cells within the biofilm were fluorescently stained with 0.1% acridine orange, and visualization was performed with a 100× objective. The control was represented by the biofilm formed in LB medium with pH 7, 10 g/L NaCl, and 0% PEG8000.

IV.2.6. The influence of abiotic stress on the cell surface hydrophobicity

The percentage of cell surface hydrophobicity of bacterial cells cultivated in NB medium at different pH values ranged between 40.25% and 66.45% (Figure IV.12). Analysis of the experimental data showed no significant differences between the percentages of cell hydrophobicity determined at pH 6, 8, and 9 compared to pH 7 (control). These results suggest that the *B. velezensis* P3.3S strain maintains a relatively constant hydrophobic character at these pH values, indicating good adaptability to acidic or alkaline conditions. Interestingly, the highest percentage of hydrophobic cells (66.45%) was recorded at pH 5. However, pH 5 did not correlate with an increase in biofilm biomass.

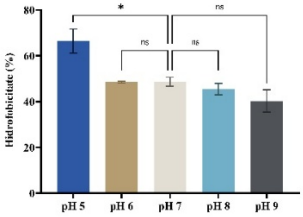

Figure IV.12. Influence of pH on the cell surface hydrophobicity of *Bacillus velezensis* P3.3S cultivated in NB medium for 24 h. The values shown represent the mean of two experimental determinations. Error bars represent the standard error of the mean. The control corresponds to the hydrophobicity percentage obtained at pH 7. Asterisks indicate significant differences (* = $p < 0.05$; ns – no significant differences).

The hydrophobicity of bacterial cells cultivated in NB medium supplemented with different NaCl concentrations ranged between 8.58% and 44.73% (Figure IV.13). A significant decrease in hydrophobicity was observed starting at a concentration of 15 g/L NaCl compared to the control (0 g/L NaCl), suggesting that saline stress negatively affects the surface properties of bacterial cells.

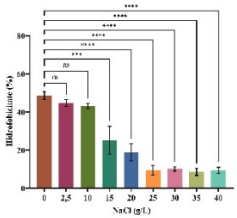

Figure IV.13. Influence of salinity on the cell surface hydrophobicity of *Bacillus velezensis* P3.3S cultivated in NB medium for 24 h. The control corresponds to the culture medium with 0 g/L NaCl. Values shown represent the mean of two experimental determinations. Error bars represent the standard error of the mean. Asterisks indicate significant differences (* = $p < 0.05$, *** = $p < 0.001$, **** = $p < 0.0001$); ns – no significant differences.

The concentrations of PEG8000 used negatively influenced the cell surface hydrophobicity, although biofilm formation was stimulated under these conditions. The percentage of hydrophobicity

decreased significantly compared to the control (0% PEG8000 – 46.49%) as the concentration of polyethylene glycol increased, reaching a minimum value of 22.02% (Figure IV.14).

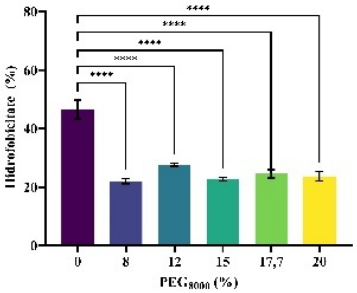

Figure IV.14. Influence of PEG8000 concentrations on the cell surface hydrophobicity of *Bacillus velezensis* P3.3S cultivated in NB medium for 24 h. The control corresponds to the culture medium with 0% PEG8000. Values shown represent the mean of two experimental determinations. Error bars represent the standard error of the mean. Asterisks indicate significant differences (**** = $p < 0.0001$).

IV.2.7. Abiotic stress does not affect the production of exopolysaccharides

The amounts of exopolysaccharides produced by the bacterial strain *B. velezensis* P3.3S cultivated in LB medium at different pH values ranged between 708 and 81.68 µg/mL (Figure IV.15). A slight increase in exopolysaccharide production was observed under acidic or alkaline conditions compared to neutral pH (pH 7), which may suggest an adaptive response of the bacteria to stress caused by pH changes.

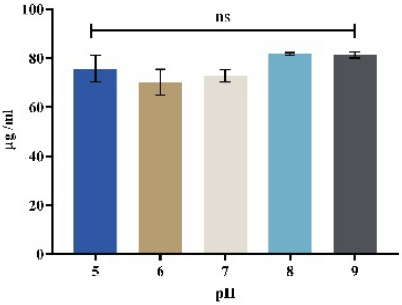

Figure IV.15. Influence of pH on the capacity of *Bacillus velezensis* P3.3S to produce exopolysaccharides during cultivation in LB medium for 48 h. The control was represented by medium at pH 7. Values represent the mean of two experimental determinations. Error bars indicate the standard error of the mean. ns – no significant differences.

When the bacterial strain *B. velezensis* P3.3S was cultivated in LB medium supplemented with different NaCl concentrations, exopolysaccharide production ranged between 52.96 and 85.95 µg/mL (Figure IV.16). Analysis of the results showed that at 2.5 g/L NaCl, the recorded amount was significantly lower compared to that at 10 g/L NaCl, which was considered the experimental control. Exopolysaccharide content increased slightly at 15 g/L NaCl and remained relatively constant as the NaCl concentration increased; however, this increase was not statistically significant compared to the control (10 g/L NaCl) – Figure IV.16.

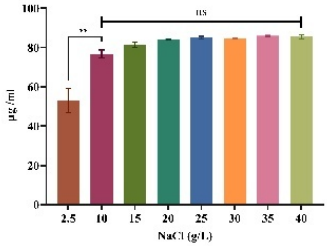

Figure IV.16. Influence of salinity on the capacity of *Bacillus velezensis* P3.3S to produce exopolysaccharides. The control was represented by medium supplemented with 10 g/L NaCl. Values represent the mean of two experimental determinations. Error bars indicate the standard error of the mean. Asterisks indicate significant differences (** = $p < 0.01$); ns – no significant differences.

Water stress induced by PEG8000 led to a slight increase in exopolysaccharide production when bacterial cells were cultivated in LB medium supplemented with PEG concentrations ≥ 8% (85.06 µg/mL) compared to the control (0% PEG8000 – 76.78 µg/mL) – Figure IV.17.

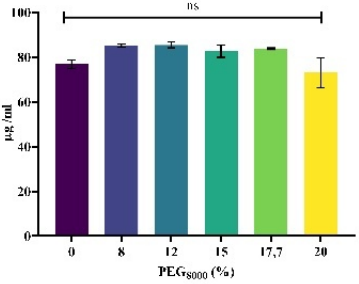

Figure IV.17. Influence of PEG on the capacity of *Bacillus velezensis* P3.3S to produce exopolysaccharides. The control was represented by medium with 0% PEG8000. Values represent the mean of two experimental determinations. Error bars indicate the standard error of the mean. ns – no significant differences.

CHAPTER V. TOLERANCE OF THE *BACILLUS SAFENSIS* P1.5S STRAIN TO ABIOTIC STRESS FACTORS AND THEIR EFFECT ON PHOSPHORUS SOLUBILIZATION POTENTIAL

V.1. Research materials and methods

Experiments conducted in this chapter were performed under abiotic stress conditions represented by pH (5 and 9), temperature (20 °C and 37 °C), and salinity (NaCl concentrations – 2.5, 10, and 15 g/L NaCl).

V.1.1. Identification of genes involved in abiotic stress tolerance and phosphorus solubilization

For the identification of genes of interest, the BLAST algorithm was used (Camacho *et al*., 2009). Genes with more than 30% identity and over 70% coverage were considered positive hits.

V.1.2. Evaluation of P1.5S strain growth in a batch culture

The effect of abiotic stress caused by pH, temperature, and salinity was assessed by monitoring the growth dynamics of *Bacillus safensis* P1.5S in a batch culture.

V.1.3. Determination of solubilized phosphorus

The ability of the P1.5S strain to solubilize tricalcium phosphate under stress conditions was evaluated using the ammonium molybdate method.

V.1.4. Growth assessment using colony counting

To establish a correlation between the amount of solubilized tricalcium phosphate and the growth of the P1.5S bacterial strain in PVK medium, the number of colony-forming units (CFU)/mL was determined.

V.1.5. Identification and quantification of organic acids by high-performance liquid chromatography

Organic acid production was evaluated by high-performance liquid chromatography (HPLC), a technique that separates components in a mixture of chemical or biological molecules based on their elution as a mobile phase (eluent) passes through a stationary phase (column) under high pressure. The separated components are detected and recorded as chromatograms (Mallik *et al*., 2016).

V.1.6. Evaluation of acid and alkaline phosphatase activities

Acid and alkaline phosphatases in the analyzed samples are capable of hydrolyzing the ester bond of para-nitrophenyl phosphate under defined conditions, producing para-nitrophenol and phosphate. In an alkaline medium, para-nitrophenol exhibits a yellow color, allowing measurement of its intensity by spectrophotometry at a wavelength of 410 nm (Artenie *et al*., 2008).

V.2. Results and discussions

V.2.1. Tolerance of *Bacillus safensis* P1.5S strain to abiotic stress

BLAST analysis revealed the presence of 56 genes that confer tolerance to pH variations, temperature fluctuations, salinity, and drought in the draft genome of the *B. safensis* P1.5S strain. The coverage percentage ranged between 80 and 100%, and the identity ranged between 30.05 and 98.46%.

Regarding the adaptation and survival of bacterial cells under extreme pH values, the draft genome of *Bacillus safensis* P1.5S contained a series of genes (15) responsible for these processes, among the most important being the atp operon composed of 8 genes (*atpABCDEFGH*).

In the draft genome of *B. safensis* P1.5S, the presence of 26 genes responsible for adaptation and survival at low temperatures (*cspB, cspC, cspD*) or high temperatures (*grpE, ywiE, groESL, dnaKJ, clpAYXPE, hrcA, ctsR, csssSR, mcsAB, rsbVW, sigAB, htrAB*) was observed.

Additionally, the draft genome of *B. safensis* P1.5S contains genes (16) that are involved when bacteria are cultivated under osmotic stress conditions, which may be caused by salinity or drought: *ftsH, lysC, pyrC, tuf, glpT, metK, yuaI, glmS, glsA1, ispH, gpmI, dapF, yugJ, yugL, metC*.

Bacteria can respond to abiotic stress by producing osmolytes. Therefore, in the draft genome of *B. safensis* P1.5S, 20 genes were identified, 5 (*proA, proB, proC/proH, proI, proJ*) are responsible for proline production, 5 (*gbsA, gbsB, opuAB, opuAC, opuD*) are involved in glycine-betaine synthesis and transport, 3 (*treA, treP, treR*) are involved in trehalose transport, and the last 7 (*gltA, gltB, gltD, gltT, gdhA, glnA, rocG*) encode glutamate synthesis.

In the genome of *B. safensis* P1.5S, 28 genes were identified that alleviate oxidative stress caused by stress factors. Of these, four genes are responsible for bacillithiol (BSH) biosynthesis, a low-molecular-weight thiol involved in the defense of bacterial cells against oxidative stress (*bshA, bshB1, bshB2, brxABC, ypd*).

Regarding antioxidant enzymes, the genome of the strain of interest contains genes responsible for the production of superoxide dismutase (*sodA*), thiol peroxidase (*tpx*), glutathione peroxidase (*bsaA/gpx*), alkyl hydroperoxide reductase (*ahpC*), bacillopeptidase (*bpr*), manganese catalase (*ydbD*), glutathione hydroxylase (*ggt*), glycolate oxidase (*glcD*), peroxiredoxin (*bcp*), catalase (*katA*), glyceraldehyde-3-phosphate dehydrogenase (*gapA* and *gapB*), anthranilate synthase (*pabA*).

The results obtained showed that incubation at 37 °C significantly improved the growth of *B. safensis* P1.5S compared to the control (28 °C) throughout the experiment, indicating an increased tolerance to high temperatures. On the other hand, lower incubation temperature (20 °C) was associated with reduced growth compared to the control (Figure V.1-A).

Investigation of the influence of pH variations on the growth of *B. safensis* P1.5S revealed significant differences between the optical densities measured after cultivation in LB medium at pH 5, pH 9, and pH 7 – control. However, the strain used showed the capacity to adapt and survive at both acidic (5) and alkaline (9) pH (Figure V.1-B).

Regarding the influence of salinity on the growth of *B. safensis* P1.5S, the results showed that this strain grown regardless of the tested NaCl concentration (2.5, 10, and 15 g/L) (Figure V.1-C).

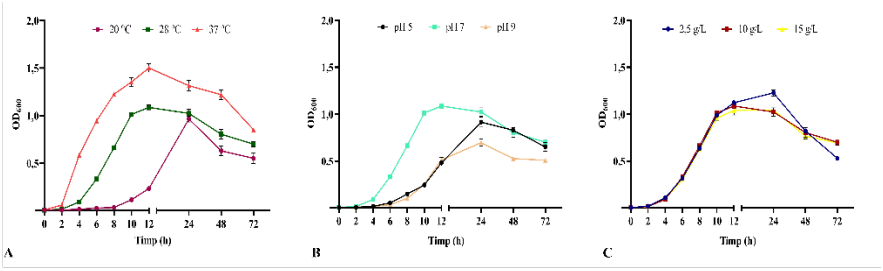

Figure V.1. Influence of temperature (A), pH (pH), and salinity (NaCl) on the growth dynamics of *B. safensis* P1.5S strain cultivated in LB medium over 72 hours. The values shown represent the mean of two experimental determinations. Error bars represent the standard error of the mean.

V.2.2. Influence of abiotic stress on the solubilization of inorganic P by *B. safensis* P1.5S

By comparatively analyzing the results regarding the effect of incubation temperature on the solubilization capacity of *B. safensis* P1.5S, it can be observed that the solubilization process was optimal at 20°C, with an increase in the amount of solubilized phosphorus at 5 and 7 days after inoculation (DAI), compared to the phosphorus values recorded after incubating the strain at 28°C (control) – Figure V.2-A. Compared to the amount of solubilized phosphorus recorded at 5 DAI after incubating the bacterial culture at 28°C (control), a significant decrease in solubilized phosphorus was observed when the strain was incubated at 37°C.

The results demonstrated that the solubilization process is dependent on the number of bacterial cells present in the PVK medium. Compared to the control (28°C), bacterial cell growth in PVK medium was stimulated when incubated at a lower temperature (20°C). This growth correlated with a more pronounced phosphorus solubilization potential at 5 and 7 DAI, compared to the phosphorus amounts determined at these time points in control. On the other hand, incubation at 37°C resulted in lower bacterial cell growth compared to the control and 20°C, showing the lowest number of viable cells present in PVK medium at 10 DAI (Figure V.2-B).

By comparatively analyzing the pH values obtained during phosphorus solubilization at different incubation temperatures, it was observed that the *B. safensis* strain caused a similar acidification of the PVK medium when incubated at 28°C and 37°C, with a single exception at 10 DAI, when the pH was significantly lower at 37°C (Figure V.2-C).

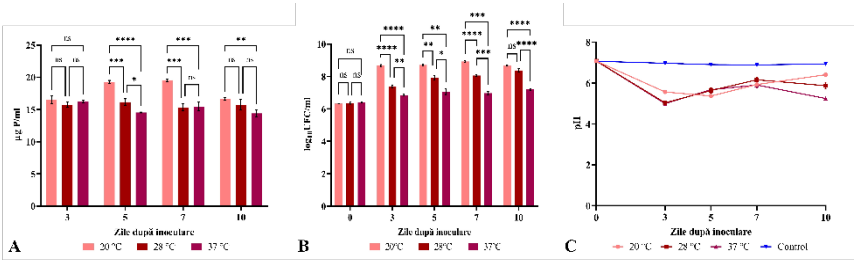

Figure V.2. Dynamics of tricalcium phosphate solubilization (A), bacterial strain growth (B), and pH variation (C) following incubation of the *Bacillus safensis* P1.5S strain at different incubation temperatures over 10 days. The control was represented by the culture incubated at 28°C in PVK medium. The values shown represent the mean of two experimental determinations. Error bars represent the standard error of the mean. The asterisk indicates significant differences (* = $p < 0.05$, ** = $p < 0.01$, *** = $p < 0.001$; **** = < 0.0001); ns – no significant differences.

Cultivation of the bacterial strain P1.5S in PVK medium with an initial pH of 7 resulted in the solubilization of phosphorus amounts ranging between 15.33 and 16.16 µg P/mL. On the other hand, when cultivated at an initial pH of 9, a higher solubilization potential was observed compared to pH 7, with determined values ranging from 14.69 to 18.73 µg P/mL. Significant differences were identified between the two tested pH values at 5 and 7 days post-inoculation, indicating an increased potential of the *Bacillus safensis* P1.5S strain to solubilize tricalcium phosphate when grown in PVK medium with an initial pH of 9 (Figure V.3-A). Regarding the growth of the P1.5S strain in PVK medium with a neutral initial pH (7), a gradual increase in colony-forming units was observed up to 10 days, with values ranging between 6.36 and 8.38 log10 CFU/mL. When inoculated in PVK medium with an alkaline initial pH (9), the maximum number of bacterial cells was identified at 10 days after inoculation (8.20 log10 CFU/mL) (Figure V.3-B). Concurrently with the phosphorus solubilization process, a decrease in the culture medium pH was observed. For both tested pH values, this parameter significantly decreased until day 3, when the minimum value was recorded, with no significant difference between the values obtained in medium with neutral or alkaline initial pH (Figure V.3-C).

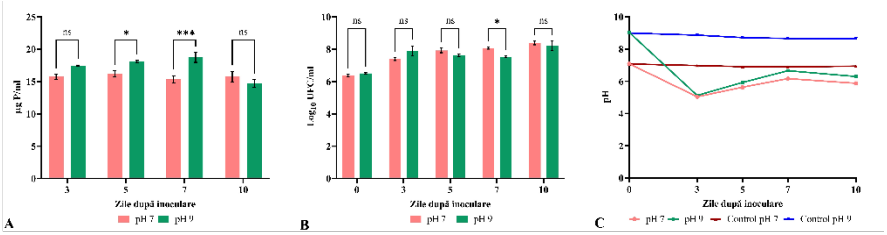

Figure V.3. Dynamics of tricalcium phosphate solubilization (A), bacterial strain growth (B), and pH variation (C) following incubation of the *Bacillus safensis* P1.5S strain in PVK medium with initial pH 7 and 9 over 10 days. The control was represented by the culture incubated at 28°C in PVK medium. Values shown represent the mean of two experimental determinations. Error bars represent the standard error of the mean. The asterisk indicates significant differences (* = $p < 0.05$, ** = $p < 0.01$, *** = $p < 0.001$; **** = < 0.0001); ns – no significant differences.

Salinity did not affect the capacity of the *Bacillus safensis* P1.5S strain to solubilize TCP in PVK broth. The amount of solubilized P ranged between 14.72 and 16.89 µg P/mL, with no significant differences observed between the control (0.150 g/L) and different NaCl concentrations (2.5 g/L, 10 g/L, and 15 g/L) (Figure V.4-A). However, increased NaCl concentrations stimulated growth at 3, 5, and 7 days after inoculation, suggesting that the P1.5S strain exhibits salinity tolerance (Figure V.4-B).

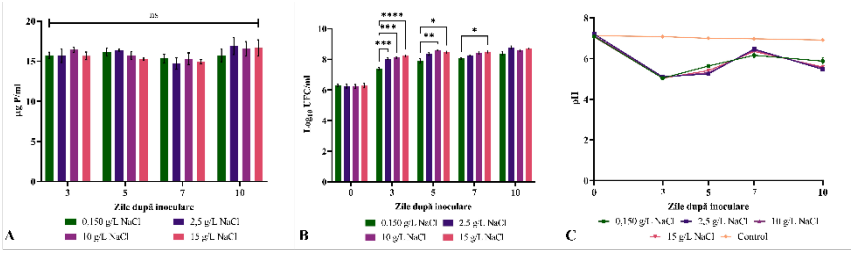

Figure V.4. Dynamics of tricalcium phosphate solubilization (A) and bacterial strain growth (B) following incubation of the *Bacillus safensis* P1.5S strain in PVK medium supplemented with different NaCl concentrations over 10 days. The control was represented by the culture incubated at 28°C in PVK medium. Values shown represent the mean of two experimental determinations. Error bars represent the standard error of the mean. The asterisk indicates significant differences (* = $p < 0.05$, ** = $p < 0.01$, *** = $p < 0.001$; **** = < 0.0001); ns – no significant differences.

V.2.3. Influence of abiotic stress factors on the mechanisms involved in solubilization

BLAST analysis of the *Bacillus safensis* P1.5S genome revealed the presence of at least 32 different genes that, according to the literature, are involved in the biosynthesis of organic acids implicated in the solubilization of insoluble phosphorus compounds (Shariati *et al*., 2017; Silva *et al*., 2021): gluconic acid (*gdh, ycdF, and kduD*), formic acid (*oxdD*), malic acid (*mdh*), citric acid (*gltA, acnA, icd), lactic acid (ldh)*, acetic acid (*poxB, aldB, pdhABCD, acsA*), and succinic acid (*sucABD, sdhABC*).

Effect of temperature on organic acid production

Comparative analysis of the results obtained at 3 days regarding the production of organic acids by the *B. safensis* P1.5S strain showed that there were no significant differences between the concentrations of acids produced at 28°C (control) and 37°C (except for citric acid, which was not produced at 28°C), a situation also observed for the amounts of phosphorus solubilized at the two temperatures. Unlike 28°C, at 20°C, tartaric and citric acids were present, although the concentrations of malic/formic, lactic, acetic, and succinic acids were higher at 28°C. Comparing the concentrations of organic acids released following incubation of the strain at 20°C and 37°C, better production of organic acids was observed at 37°C. However, the phosphorus amounts determined at the two temperatures were not statistically different.

Comparison of the concentrations of organic acids produced at 5 days showed that cultivation of *B. safensis* P1.5S at 20°C resulted in higher values for oxalic and malic acids compared to 28°C and 37°C. The difference in concentration between these acids could explain why the phosphorus amount is higher at 20°C, as these two acids are considered the most efficient in solubilizing phosphorus compounds based on their acidity constant. Moreover, all seven organic acids were produced at this temperature, whereas at 37°C tartaric acid was not detected, and at 28°C citric and acetic acids were not produced, explaining the significant difference in phosphorus content determined. No significant differences were observed in the phosphorus amounts recorded at 28°C and 37°C, although the concentrations of organic acids produced at these temperatures were different. At 28°C, higher values of oxalic, tartaric/gluconic, lactic, and succinic acids were obtained compared to 37°C. On the other hand, at 37°C, higher concentrations of malic/formic, citric, and acetic acids were observed compared to 28°C. At 7 days post-inoculation, no significant differences were observed between the concentrations of oxalic, malic/formic, citric, lactic, and acetic acids synthesized at 28°C and 37°C. The only differences between the two tested temperatures were for succinic acid, which was produced in a higher concentration at 28°C, while the content of tartaric/gluconic acid was higher at 37°C, and therefore no differences could be established in the phosphorus amounts solubilized by *B. safensis* P1.5S at these two temperatures. At 20°C, the highest phosphorus amount and the highest number of

bacterial cells were recorded, although in some cases the concentrations of organic acids were lower (as with tartaric/gluconic, acetic, and succinic acids) or there were no significant differences (oxalic, malic/formic, citric, and lactic acids) compared to 28°C and 37°C. As mentioned earlier, it is possible that the organic acids produced at 20°C were subsequently used as an energy source, since the number of bacterial cells in the PVK medium was the highest compared to the other temperatures. At 37°C, the cell number in the medium was the lowest, yet some organic acids were produced in higher concentrations compared to 28°C and 20°C.

Comparative analysis of the organic acid concentrations produced at 10 days at the three tested temperatures revealed no significant differences in malic/formic and citric acid concentrations, which are considered the strongest acids according to their acidity constant. Lactic acid was no longer detected in the supernatant of any of the cultures incubated at the three temperatures. Differences in concentration were observed for oxalic acid (highest at 20°C), tartaric acid (not detected at 20°C, highest at 37°C), acetic acid (produced in similar concentrations at 37°C and 28°C), and succinic acid (highest at 28°C, followed by 20°C). At 10 days after inoculation, the phosphorus amounts determined were not statistically different, which can be attributed to the variation in organic acid concentrations.

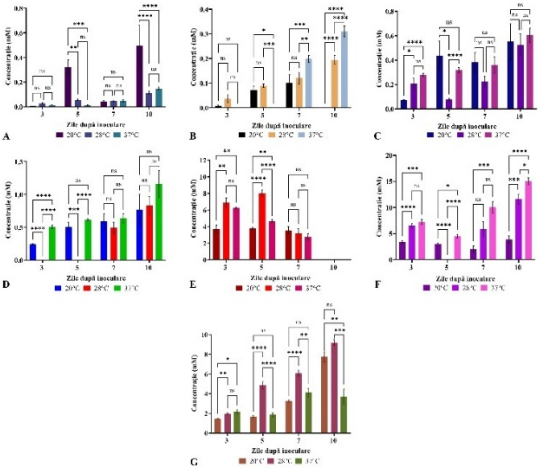

Figure V.5. Influence of temperature on organic acid production by the *Bacillus safensis* P1.5S strain cultivated in PVK medium over 10 days of incubation: A – oxalic acid; B – tartaric/gluconic acid; C – malic/formic acid; D – citric acid; E – lactic acid; F – acetic acid; G – succinic acid. The control was represented by the culture incubated in PVK medium at 28°C. The values shown represent the mean of two experimental determinations. Error bars represent the standard error of the mean. Asterisks indicate significant differences (* = $p < 0.05$, ** = $p < 0.01$, *** = $p < 0.001$; **** = < 0.0001); ns – no significant differences.

Effect of pH on organic acid production

Comparing the organic acids produced at an initial pH of 7 (control) and 9, it was observed that 3 days after inoculation of *Bacillus safensis* P1.5S in PVK medium, five organic acids were produced: oxalic, malic/formic, lactic, acetic, and succinic, in concentrations that were not statistically different. The lack of significant differences between the concentrations of organic acids synthesized at pH 7 and 9 was also observed for the amounts of solubilized P, bacterial cell numbers, and medium pH.

At 5 days after inoculation, five organic acids were detected at both pH 7 and pH 9, but two of these acids differed depending on the tested pH. The acids produced at both initial pH values were oxalic, lactic, and succinic. Additionally, at pH 7, malic/formic and tartaric/gluconic acids were present, while at pH 9, citric and acetic acids were also identified. Data on the concentrations of the acids produced showed no significant differences for oxalic, lactic, and succinic acids at pH 7 and 9. However, citric and acetic acids produced at pH 9 were present in higher concentrations compared to those released in the control. Moreover, citric acid is a tricarboxylic acid considered strong and effective in phosphate solubilization. This may explain the higher amount of solubilized phosphorus observed at pH 9 compared to pH 7.

At 7 days after inoculation, eight organic acids were produced regardless of the initial pH: oxalic, tartaric/gluconic, malic/formic, citric, lactic, acetic, succinic, and an unknown acid. Oxalic and succinic acids were produced in higher concentrations at pH 9, while the concentration values of the other acids were not statistically different. Cultivation of the strain in PVK medium at pH 9 likely led to greater phosphate solubilization due to the higher concentrations of oxalic and succinic acids compared to the control.

In the final measurement (10 DAI), although there was no significant difference in the solubilized phosphorus content between pH 7 and pH 9, variations in organic acid synthesis were observed. Lactic acid was detected only at an initial pH of 9, while oxalic, acetic, and succinic acids were produced in higher concentrations at pH 9 compared to pH 7. Conversely, malic/formic acid showed a higher concentration in the control.

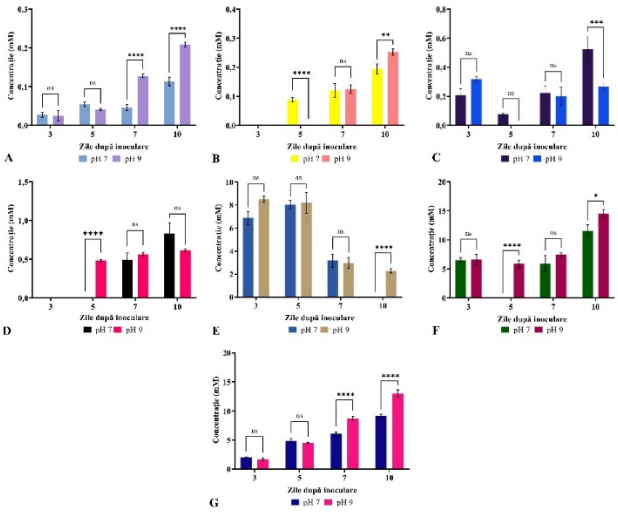

Figure V.6. Effect of pH on the production of organic acids by *Bacillus safensis* P1.5S cultivated in PVK medium over 10 days of incubation: A – oxalic acid; B – tartaric/gluconic acid; C – malic/formic acid; D – citric acid; E – lactic acid; F – acetic acid; G – succinic acid. The control was represented by the culture incubated in PVK medium at an initial pH of 7. Values represent the mean of two experimental determinations. Error bars indicate the standard error of the mean. Asterisks denote significant differences (** = $p < 0.01$, *** = $p < 0.001$; **** = < 0.0001); ns – no significant differences.

Efect of salinity on organic acid production

Comparative analysis of HPLC chromatograms showed that the synthesis and release of organic acids varied depending on the NaCl concentrations used to supplement the PVK medium. At the beginning of the incubation period (3 days after inoculation, DAI), the three main organic acids (lactic, acetic, and succinic) were produced at all tested salt concentrations. However, salt stress induced a different pattern of acid release. *Bacillus safensis* P1.5S produced more acetic acid under saline stress compared to the control (0.150 g/L NaCl), where lactic acid was released as the predominant acid. Additionally, citric acid was detected only at the highest NaCl concentration tested (15 g/L), while tartaric/gluconic and malic/formic acids were not detected at this concentration. Oxalic acid was detected in PVK broth supplemented with various NaCl concentrations, except at 10 g/L NaCl.

At 5 DAI, lactic acid production decreased with increasing NaCl concentration in PVK medium. Similar to the control, acetic acid was not detected at 10 g/L NaCl, but it was present at 2.5 and 15 g/L NaCl (6.03 mM and 4.72 mM, respectively). Salinity inhibited succinic and oxalic acid

production but stimulated the release of tartaric/gluconic acids, with the highest concentration observed at 10 g/L NaCl (0.432 mM).

At 7 DAI, citric, lactic, and succinic acids were synthesized regardless of NaCl concentration. Acetic and oxalic acids were not detected in PVK medium supplemented with 10 g/L NaCl, although both acids were present in all other samples.

By the end of the incubation period (10 DAI), increased salt concentrations inhibited the production of oxalic, malic/formic, citric, and acetic acids, but stimulated the release of tartaric/gluconic acid (especially at 10 g/L NaCl). At 15 g/L NaCl, tartaric/gluconic and malic/formic acids were not detected.

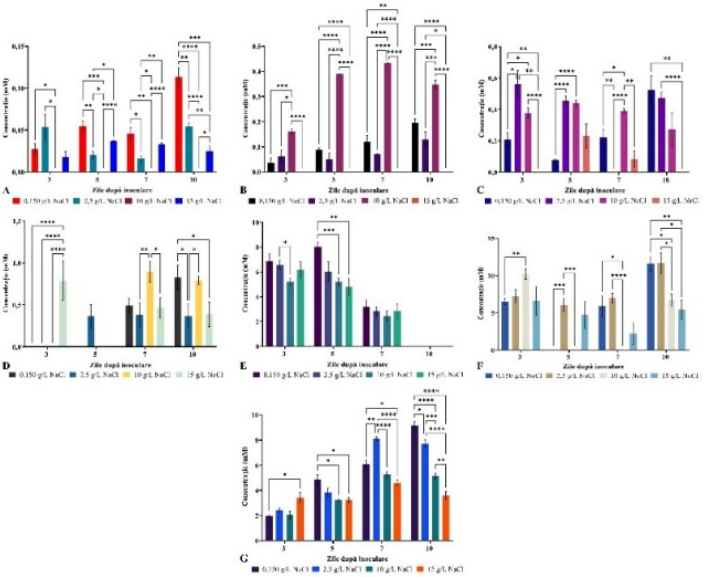

Figure V.7. Influence of NaCl concentrations on the production of organic acids by the *Bacillus safensis* P1.5S strain cultivated in PVK medium: A – oxalic acid; B – tartaric/gluconic acid; C – malic/formic acid; D – citric acid; E – lactic acid; F – acetic acid; G – succinic acid. The control was represented by the culture incubated in PVK medium containing 0.150 g/L NaCl. The values shown represent the mean of two experimental determinations. Error bars represent the standard error of the mean. Asterisks indicate significant differences (* = $p < 0.05$, ** = $p < 0.01$, *** = $p < 0.001$; **** = < 0.0001).

V.2.3.2. Acid and alkaline phosphatase activity produced by *Bacillus safensis* P1.5S under stress conditions

BLAST analysis revealed the presence of ten genes encoding acid and alkaline phosphatase synthesis (*ycsE, yitU, phoABPR, suhB, prpC, acpA, yqeG*).

Effect of temperature on acid and alkaline phosphatase activity

The results showed that incubation temperature significantly influenced the activity of acid and alkaline phosphatases produced by *B. safensis* P1.5S. At several time points, the activity of both enzymes increased at 20°C and 37°C compared to the control (28°C). Maximum activity (180.456 nmol pNP/mL/h for acid phosphatase and 157.867 nmol pNP/mL/h for alkaline phosphatase) was recorded at 10 days after inoculation (DAI) in cultures incubated at 20°C. Acid phosphatase activity increased at 3 and 10 DAI when incubated at 20°C, whereas incubation at a higher temperature (37°C) enhanced activity at 5 DAI (Figure V.16-A). No significant differences in acid phosphatase activity were observed at 7 DAI across the tested temperatures. For alkaline phosphatase, higher activity was observed at 3 and 5 DAI when incubated at 37°C compared to the control (28°C).

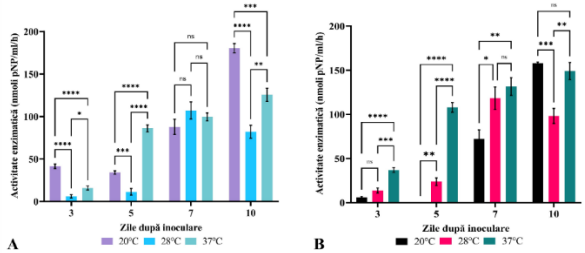

Figure V.7. Influence of temperature on acid phosphatase (A) and alkaline phosphatase (B) activity produced by *Bacillus safensis* P1.5S cultivated in PVK medium over 10 days. The control represents the culture incubated at 28°C. Values are the mean of two experimental determinations. Error bars represent the standard error of the mean. Asterisks indicate significant differences (* = $p < 0.05$, ** = $p < 0.01$, *** = $p < 0.001$, **** = $p < 0.0001$); ns – no significant differences.

Effect of pH on Acid and Alkaline Phosphatase Activity

The results indicated that alkalinity did not significantly alter the dynamics of acid and alkaline phosphatase production during cultivation of *B. safensis* P1.5S in PVK medium adjusted to pH 9. Activity of both enzymes increased slightly at pH 9 at 3 and 5 DAI compared to the control (pH 7).

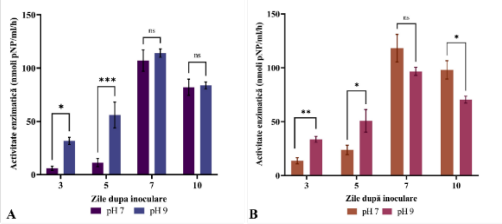

Figure V.9. Influence of pH on acid phosphatase (A) and alkaline phosphatase (B) activity produced by *Bacillus safensis* P1.5S. The control represents the culture incubated in PVK medium with an initial pH of 7.

Values are the mean of two experimental determinations. Error bars represent the standard error of the mean. Asterisks indicate significant differences (* = $p < 0.05$, ** = $p < 0.01$, *** = $p < 0.001$); ns – no significant differences.

Effect of Salinity on Acid and Alkaline Phosphatase Activity

Salinity did not affect acid or alkaline phosphatase activity over the 10-day incubation period (Figure V.9). The only significant difference was observed for acid phosphatase at 5 DPI, where higher NaCl concentrations inhibited enzymatic activity. Alkaline phosphatase activity showed no statistical differences when *B. safensis* P1.5S was cultured in PVK medium supplemented with 2.5, 10, and 15 g/L NaCl compared to the control (0.150 g/L NaCl).

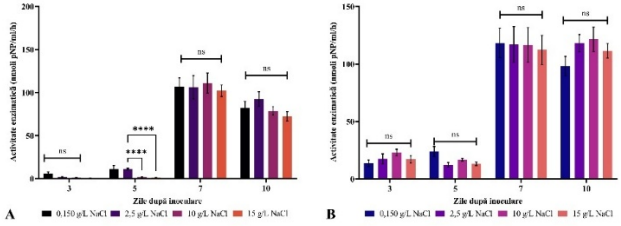

Figure V.9. Influence of salinity on acid phosphatase (A) and alkaline phosphatase (B) activity produced by *Bacillus safensis* P1.5S. The control represents the culture incubated in PVK medium containing 0.150 g/L NaCl. Values are the mean of two experimental determinations. Error bars represent the standard error of the mean. Asterisks indicate significant differences (*** = $p < 0.001$); ns – no significant differences.

CONCLUSIONS

- Literature analysis highlighted that climate change negatively affects plant growth and development, as well as rhizospheric bacteria.
- Plant-associated rhizosphere bacteria can employ direct and indirect mechanisms to stimulate plant growth and alleviate abiotic stress.
- Abiotic stress-tolerant bacteria produce osmolytes, antioxidants, and extracellular polymeric substances to adapt and survive under unfavorable conditions.
- The efficiency of beneficial bacteria depends on successful root colonization through complex mechanisms such as chemotaxis, motility, quorum sensing, and biofilm formation.
- Screening for plant growth-promoting mechanisms identified strains P3.3S and P1.5S as having multiple beneficial traits.
- The draft genome of strain P3.3S is 3,860,972 bp, while that of P1.5S is smaller at 3,667,318 bp.
- The assembled genomes are available in NCBI GenBank under accession numbers JARXQM000000000 (P3.3S) and JARZFW000000000 (P1.5S).
- Strains P3.3S and P1.5S were identified as *Bacillus velezensis* and *Bacillus safensis*, respectively, based on dDDH values.
- Functional genome annotation predicted 3,826 genes for *B. velezensis* P3.3S and 3,748 genes for *B. safensis* P1.5S.
- AntiSMASH analysis of P3.3S identified gene clusters for polyketides (bacillaene, difficidin, bacilysin, macrolactin H), lipopeptides (surfactin, fengycin, bacillomycin, iturin), and the siderophore bacillibactin.
- P1.5S genome analysis revealed biosynthetic gene clusters for polyketides (bacilysin), lipopeptides (surfactin, lichenysin), siderophores (bacillibactin, schizokinen), and botromicin A2.
- MALDI-TOF mass spectrometry showed that P3.3S produces antifungal lipopeptides (surfactin, iturin, fengycin), while P1.5S produces only surfactin and bacillibactin.
- P3.3S exhibited antimicrobial activity against plant pathogens: *Agrobacterium tumefaciens*, *Rhizoctonia solani*, *Fusarium oxysporum*, *Sclerotinia sclerotiorum*, and *Verticillium dahliae*, whereas P1.5S inhibited only *R. solani*.
- P3.3S maintained antimicrobial activity under stress conditions: pH (5–8), NaCl (2.5–35 g/L), and PEG8000 (8–20%).
- P3.3S genome contains genes involved in biofilm formation, chemotaxis, motility, quorum sensing, and extracellular polymeric substance production.

- P3.3S showed chemotactic responses (≥2) to tested compounds (glucose, fumaric acid, citric acid, maltose, malic acid, fructose, succinic acid).
- Motility of P3.3S was not affected by stress factors.
- P3.3S adhered strongly and formed biofilms under acidic and alkaline pH, as well as varying NaCl and PEG concentrations.
- Biofilm architecture varied with cultivation conditions, showing a spongy network at low salinity/PEG and dense chains at higher PEG concentrations.
- Cell surface hydrophobicity was negatively influenced by salinity and drought stress.
- Stress conditions did not affect exopolysaccharide production in P3.3S.
- P1.5S genome contains genes for stress tolerance (extreme temperatures, pH variation, salinity, drought) and for producing osmolytes and antioxidants.
- P1.5S tolerated abiotic stress: pH (5, 7, 9), NaCl (2.5–15 g/L), and temperatures (20, 28, 37°C).
- P1.5S solubilized tricalcium phosphate regardless of stress conditions, indicating tolerance to temperature, alkaline pH, and salinity.
- P1.5S genome includes genes for producing organic acids (gluconic, malic, formic, citric, lactic, acetic, succinic) and phosphatases.
- Under stress, P1.5S solubilizes tricalcium phosphate mainly via production of organic acids (tartric/gluconic, malic/formic, citric, lactic, acetic, succinic, and an unknown acid).
- The type and concentration of organic acids change depending on stress (pH, temperature, salinity) but do not significantly affect phosphate solubilization efficiency.
- Acid and alkaline phosphatases produced by P1.5S do not contribute to tricalcium phosphate solubilization under alkaline pH, temperature, or salinity stress.
- The results demonstrate the biotechnological potential of both bacterial strains, suggesting their use as biofertilizers or biopesticides.
- Further studies are needed to fully assess the long-term effects of abiotic stress on strain viability and efficiency, their interactions with soil microbial populations, field performance, and environmental risk assessment in agricultural ecosystems.

FUTURE RESEARCH PERSPECTIVES

1. The results obtained in this doctoral thesis encourage further research on bacteria–plant interactions under abiotic stress conditions. In this regard, the following directions are planned:
2. Testing the two *Bacillus sp.* strains to identify other plant growth-promoting mechanisms, such as the production of volatile organic compounds and the ability to fix atmospheric nitrogen.
3. Evaluating the behavior of *Bacillus safensis* P1.5S under combinations of long-term abiotic stress factors.
4. Investigating the mechanisms involved in root colonization by *Bacillus safensis* P1.5S (chemotaxis, motility, biofilm formation, exopolysaccharide production).
5. Confirming in vitro the mechanisms of abiotic stress tolerance, such as the production of osmolytes and antioxidant enzymes.
6. Testing the strains' ability to promote plant growth under greenhouse and field conditions.
7. Analyzing the expression of genes involved in stress adaptation and plant growth promotion.
8. Confirming the ability of *Bacillus velezensis* P3.3S to produce polyketides, such as bacillaene, difficidin, macrolactin H, and bacilysin.
9. Investigating the influence of combinations of stress factors on the root colonization mechanisms of *Bacillus velezensis* P3.3S.
10. Testing the biocontrol potential of *Bacillus velezensis* P3.3S on plants infected with various phytopathogenic fungi.
11. Evaluating the effect of stress factors on the biosynthesis of antimicrobial secondary metabolites by *Bacillus velezensis* P3.3S.

DISSEMINATION OF THE RESEARCH FINDINGS

List of publications

1. **Loredana-Elena Mantea**, Amada El-Sabeh, Marius Mihășan, Marius Ștefan (2025). *Bacillus safensis* P1.5S exhibits phosphorus-solubilizing activity under abiotic stress. *Horticulturae*, *11*, 388. https://doi.org/10.3390/horticulturae11040388 (**Q1**, **IF 3,1**).
2. **Loredana-Elena Mantea,** Cristina-Veronica Moldovan, Mihaela Savu, Laura Gabriela Sârbu, Marius Ștefan, Mihail Lucian Bîrsă (2024). An eco-friendly method to synthesize potent antimicrobial tricyclic flavonoids. *Antibiotics*, *13*(9), 798; https://doi.org/10.3390/antibiotics13090798 (**Q1**, **IF 4,3**).
3. Cristina-Veronica Moldovan, **Loredana-Elena Mantea**, Mihaela Savu, Peter G Jones, Laura Gabriela Sarbu, Marius Stefan, Mihail Lucian Bîrsă (2024). Novel tricyclic flavonoids as promising anti-MRSA agents. *Pharmaceuticals*, *17*(10), 1276; https://doi.org/10.3390/ph17101276 (**Q1**, **IF 4,3**).

Contributions to international databases

1. The raw data generated from Illumina sequencing of the genomes of *Bacillus safensis* P1.5S and *Bacillus velezensis* P3.3S have been deposited in the NCBI Sequence Read Archive (SRA) under the accession numbers SRX20079035 and SRX20032234, respectively.
2. The assembled genomes of the two strains have been submitted to NCBI Genome with the following accession numbers:
   - *Bacillus safensis* P1.5S: ASM2993051v1, corresponding to GenBank assembly GCA_029930515.1 and RefSeq assembly GCF_029930515.1.
   - *Bacillus velezensis* P3.3S: ASM2988806v1, corresponding to GenBank assembly GCA_029888065.1 and RefSeq assembly GCF_029888065.1.

List of published abstracts

1. **Loredana-Elena Mantea**, Amada El-Sabeh, Theo Daboudet, Marius Mihășan, Francois Krier, Marius Stefan (2023). Genomic and functional analysis of *Bacillus velezensis* P3.3S – a putative biocontrol agent of plant pathogens. *FEBS Open Bio 13* (Suppl. S2) pag 44-45. DOI: 10.1002/2211-5463.13645 (**IF 2,792**).
2. **Loredana-Elena Mantea**, Ștefan Olaru, Marius Mihășan, Francois Krier, Marius Ștefan (2023). Biofilm formation under abiotic stress by *Bacillus velezensis* P3.3S – a plant growth promoting bacteria. *Journal of Experimental and Molecular Biology* 24(4):245 DOI: 10.47743/jemb-2023-24-4.

3. **Loredana-Elena Mantea**, Francois Krier, Marius Ștefan – The antimicrobial activity of P3.3S strain against *Agrobacterium tumefaciens* and *Rhizoctonia solani.* (2022). *Journal of Experimental and Molecular Biology 23*(2):59 DOI:10.47743/jemb-2022-23-2.
4. **Loredana-Elena Mantea**, Marius Mihășan, Marius Ștefan (2021). Organic acids production by phosphate solubilizing bacteria. *Journal of Experimental and Molecular Biology* 22(2):52, DOI:10.47743/jemb-2021-5.
5. **Loredana-Elena Mantea**, Marius Ștefan (2021). The influence of abiotic factors on phosphate solubilizing bacteria. *Studia Universitatis Babeş-Bolyai Biologia 66*(1):21-22 DOI:10.24193/subbbiol.2021.1.03.
6. **Loredana-Elena Mantea**, Marius Ștefan (2021). The effect of pH and temperature on phosphate solubilization potential and growth of a bacterial strain isolated from maize rhizosphere. *Genetics and Applications* p. 68 ISSN 2566-431x.

Participation in international conferences

1. **Loredana-Elena Mantea**, Amada El-Sabeh, Theo Daboudet, Marius Mihășan, Francois Krier, Marius Stefan. Genomic and functional analysis of *Bacillus velezensis* P3.3S – a putative biocontrol agent of plant pathogens. The 47th FEBS Congress 2023 – Together in bioscience for a better future. 8-12 july, Tours, France. Speed talk and Poster.
2. **Loredana-Elena Mantea**, Amada El-Sabeh, Marius Mihășan, Marius Ștefan. Genomic characterization of *Bacillus velezensis* P3.3S. RoBioinfo Conference 2023, 11-13 may, Bucharest, Romania. Poster.
3. **Loredana-Elena Mantea**, Marius Ștefan. Phosphate solubilizing bacteria ability to form biofilm under abiotic stress. International Union of Microbiological Societies (IUMS) Hybrid Congress 2022, 20-22 july, Rotterdam, Olanda/Online. Poster.
4. **Loredana-Elena Mantea**, Marius Ștefan. The influence of abiotic factors on phosphate solubilizing bacteria. The 6th Young Researchers in BioSciences International Symposium 2021, 22-25 july, Cluj-Napoca, România. Oral Presentation.
5. **Loredana-Elena Mantea**, Marius Ștefan. The effect of pH and temperature on phosphate solubilization potential and growth of a bacterial strain isolated from maize rhizosphere. The third International Green Biotechnology Congress 2021, 30 september – 2 october, Sarajevo, Bosnia and Herzegovina. Poster.

Participations in national conferences

1. Loredana-Elena Mantea, Amada El-Sabeh, Marius Mihășan, Francois Krier, Marius Ștefan. *Bacillus velezensis* P3.3S – a putative bacterial biocontrol agent. Conference: Ecology and Ecosystem Protection, the XIV Edition, 2023, 2-4 november, Bacău, Romania. Poster

2. **Loredana-Elena Mantea**, Ștefan Olaru, Marius Mihășan, Francois Krier, Marius Ștefan. Biofilm formation under abiotic stress by *Bacillus velezensis* P3.3S – a plant growth promoting bacteria. 2023, Scientific Session of the Faculty of Biology: Trends in Biology: from molecules to complex systems. 2023, October 27–28, Iași, Romania. Poster.
3. **Loredana-Elena Mantea**, Francois Krier, Marius Ștefan – The antimicrobial activity of P3.3S strain against *Agrobacterium tumefaciens* and *Rhizoctonia solani.* Scientific Session of the Faculty of Biology: Trends in Biology: From Molecules to Complex Systems. 2022, October 27–28, Iași, Romania. Oral Presentation.
4. **Loredana-Elena Mantea**, Marius Mihășan, Marius Ștefan. Organic acids production by phosphate solubilizing bacteria. Scientific Session of the Faculty of Biology: Trends in Biology: From Molecules to Complex Systems. 2023, October 28–29, Iași, Romania. Oral Presentation.
5. **Loredana-Elena Mantea**, Marius Ștefan. The effect of ph and temperature on phosphate-solubilizing bacteria. Annual Scientific Session of Natural Science Students, 5th Edition, Iași, May 22, 2021. Oral Presentation.
6. **Loredana-Elena Mantea**, Marius Ștefan. Influence of abiotic factors on the ability of rhizosphere microorganisms to solubilize inorganic phosphorus. Annual Scientific Session of Natural Science Students, 4th Edition, Iași, October 31, 2020. Oral Presentation.

International Scholarships Awarded:

Scholarship for Young Researchers at the 47th FEBS Congress, July 8–12, 2023, Tours, France.

REFERENCES

1. Aarab, S., Ollero, J., Megías, M., Laglaoui, A., Bakkali, M., Arakrak, A. (2019). Some characteristics of phosphate solubilizing rhizobacteria as an ecological strategy for sustainable agriculture. *Materials Today: Proceedings*, *13*, 1224–1228.
2. Ahmad, H. M., Fiaz, S., Hafeez, S., Zahra, S., Shah, A. N., Gul, B., Aziz, O., Mahmood-Ur-Rahman, Fakhar, A., Rafique, M., Chen, Y., Yang, S. H., Wang, X. (2022). Plant growth-promoting rhizobacteria eliminate the effect of drought stress in plants: A review. In *Frontiers in Plant Science*, *13*.
3. Ali, S., Glick, B. R. (2019). Plant–bacterial interactions in management of plant growth under abiotic stresses. In J. Singh (Ed.), *New and Future Developments in Microbial Biotechnology and Bioengineering* (pp. 21–45). Elsevier.
4. Ansari, F. A., Ahmad, I. (2018). Biofilm development, plant growth promoting traits and rhizosphere colonization by *Pseudomonas entomophila* FAP1: A promising PGPR. *Advances in Microbiology*, *08*(03), 235–251.
5. Aroney, S. T. N., Poole, P. S., Sánchez-Cañizares, C. (2021). Rhizobial chemotaxis and motility systems at work in the soil. *Frontiers in Plant Science*, *12*, 1–15.
6. Arora, N. K. (2019). Impact of climate change on agriculture production and its sustainable solutions. *Environmental Sustainability*, *2*(2), 95–96.
7. Artenie, V., Ungureanu, E., Negură, A. M. (2008). *Metode de investigare a metabolismului glucidic şi lipidic*. PIM Iaşi.
8. Awais, M., Tariq, M., Ali, A., Ali, Q., Khan, A., Tabassum, B., Nasir, I. A., Husnain, T. (2017). Isolation, characterization and inter-relationship of phosphate solubilizing bacteria from the rhizosphere of sugarcane and rice. *Biocatalysis and Agricultural Biotechnology*, *11*, 312–321.
9. Aziz, R. K., Bartels, D., Best, A., DeJongh, M., Disz, T., Edwards, R. A., Formsma, K., Gerdes, S., Glass, E. M., Kubal, M., Meyer, F., Olsen, G. J., Olson, R., Osterman, A. L., Overbeek, R. A., McNeil, L. K., Paarmann, D., Paczian, T., Parrello, B., … Zagnitko, O. (2008). The RAST Server: Rapid annotations using subsystems technology. *BMC Genomics*, *9*.
10. Balestrini, R., Lumini, E., Borriello, R., Bianciotto, V. (2015). Plant-soil biota interactions. In *Soil Microbiology, Ecology and Biochemistry* (pp. 311–338). Elsevier.
11. Bankevich, A., Nurk, S., Antipov, D., Gurevich, A. A., Dvorkin, M., Kulikov, A. S., Lesin, V. M., Nikolenko, S. I., Pham, S., Prjibelski, A. D., Pyshkin, A. V., Sirotkin, A. V., Vyahhi, N., Tesler, G., Alekseyev, M. A., Pevzner, P. A. (2012). SPAdes: A new genome assembly algorithm and its applications to single-cell sequencing. *Journal of Computational Biology*, *19*(5), 455–477.

12. Behera, B. C., Singdevsachan, S. K., Mishra, R. R., Dutta, S. K., Thatoi, H. N. (2014). Diversity, mechanism and biotechnology of phosphate solubilising microorganism in mangrove-A review. *Biocatalysis and Agricultural Biotechnology*, *3*(2), 97–110.
13. Bhagat, N., Raghav, M., Dubey, S., Bedi, N. (2021). Bacterial exopolysaccharides: Insight into their role in plant abiotic stress tolerance. *Journal of Microbiology and Biotechnology*, *31*(8), 1045–1059.
14. Blin, K., Shaw, S., Augustijn, H. E., Reitz, Z. L., Biermann, F., Alanjary, M., Fetter, A., Terlouw, B. R., Metcalf, W. W., Helfrich, E. J. N., Van Wezel, G. P., Medema, M. H., Weber, T. (2023). AntiSMASH 7.0: New and improved predictions for detection, regulation, chemical structures and visualisation. *Nucleic Acids Research*, *51*(W1), W46–W50.
15. Bridier, A., Meylheuc, T., Briandet, R. (2013). Realistic representation of *Bacillus subtilis* biofilms architecture using combined microscopy (CLSM, ESEM and FESEM). *Micron*, *48*, 65–69.
16. Calvin, K., Dasgupta, D., Krinner, G., Mukherji, A., Thorne, P. W., Trisos, C., Romero, J., Aldunce, P., Barrett, K., Blanco, G., Cheung, W. W. L., Connors, S., Denton, F., Diongue-Niang, A., Dodman, D., Garschagen, M., Geden, O., Hayward, B., Jones, C., … Ha, M. (2023). *IPCC, 2023: Climate Change 2023: Synthesis Report. Contribution of Working Groups I, II and III to the Sixth Assessment Report of the Intergovernmental Panel on Climate Change [Core Writing Team, H. Lee and J. Romero (eds.)]. IPCC, Geneva, Switzerland.*
17. Camacho, C., Coulouris, G., Avagyan, V., Ma, N., Papadopoulos, J., Bealer, K., Madden, T. L. (2009). BLAST+: Architecture and applications. *BMC Bioinformatics*, *10*.
18. Cao, Y., Pi, H., Chandrangsu, P., Li, Y., Wang, Y., Zhou, H., Xiong, H., Helmann, J. D., Cai, Y. (2018). Antagonism of two plant-growth promoting *Bacillus velezensis* isolates against *Ralstonia solanacearum* and *Fusarium oxysporum*. *Scientific Reports*, *8*(1).
19. Chen, L., Liu, Y. (2024). The function of root exudates in the root colonization by beneficial soil rhizobacteria. *Biology*, *13*(2).
20. Dong, X., Tu, C., Liu, Y., Zhang, R., Liu, Y. (2022). Identification of the core c-di-GMP turnover proteins responsible for root colonization of *Bacillus velezensis*. *IScience*, *25*(11).
21. Fageria, N. K., Moreira, A. (2011). The role of mineral nutrition on root growth of crop plants. *Advances in Agronomy*, *110*.
22. FAO. (2017). The future of food and agriculture and challenges.
23. FAO, I. U. W. W. (2019). The state of food security and nutrition in the world : safeguarding against economic slowdowns and downturns. *Food and Agriculture Organization of the United Nations.*

24. Fessia, A., Sartori, M., García, D., Fernández, L., Ponzio, R., Barros, G., Nesci, A. (2022). In vitro studies of biofilm-forming *Bacillus* strains, biocontrol agents isolated from the maize phyllosphere. *Biofilm*, *4*.
25. Flissi, A., Ricart, E., Campart, C., Chevalier, M., Dufresne, Y., Michalik, J., Jacques, P., Flahaut, C., Lisacek, F., Leclère, V., Pupin, M. (2019). Norine: Update of the nonribosomal peptide resource. *Nucleic Acids Research*, *48*(D1), D465–D469.
26. Gai, Y., Wang, H. (2024). Plant Disease: A Growing Threat to Global Food Security. In *Agronomy*, *14*(8).
27. Gang, S., Sharma, S., Saraf, M., Buck, M., Schumacher, J. (2019). Analysis of indole-3-acetic acid (IAA) production in Klebsiella by LC-MS/MS and the Salkowski method. *Bio-Protocol*, *9*(9), 1–9.
28. Gouda, S., Kerry, R. G., Das, G., Paramithiotis, S., Shin, H. S., Patra, J. K. (2018). Revitalization of plant growth promoting rhizobacteria for sustainable development in agriculture. *Microbiological Research*, *206*, 131–140.
29. Gregory, G. J., Boyd, E. F. (2021). Stressed out: Bacterial response to high salinity using compatible solute biosynthesis and uptake systems, lessons from Vibrionaceae. In *Computational and Structural Biotechnology Journal*, *19*, 1014–1027.
30. Hakim, S., Naqqash, T., Nawaz, M. S., Laraib, I., Siddique, M. J., Zia, R., Mirza, M. S., Imran, A. (2021). Rhizosphere engineering with plant growth-promoting microorganisms for agriculture and ecological sustainability. *Frontiers in Sustainable Food Systems* (Vol. 5).
31. Haque, M. M., Mosharaf, M. K., Khatun, M., Haque, M. A., Biswas, M. S., Islam, M. S., Islam, M. M., Shozib, H. B., Miah, M. M. U., Molla, A. H., Siddiquee, M. A. (2020). Biofilm producing rhizobacteria with multiple plant growth-promoting traits promote growth of tomato under water-deficit stress. *Frontiers in Microbiology*, *11*.
32. Keren, G., Yehezkel, G., Satish, L., Adamov, Z., Barak, Z., Ben-Shabat, S., Kagan-Zur, V., Sitrit, Y. (2024). Root-secreted nucleosides: signaling chemoattractants of rhizosphere bacteria. *Frontiers in Plant Science*, *15*.
33. Khadraji, A., Mouradi, M., Bassour, H., Ghoulam, C. (2017). Phosphate solubilization capacity , salinity and drought tolerance of rhizobia nodulating chickpea (*Cicer arietinum* L .). *Moroccan Journal of Chemistry*, *4*(5), 722–729.
34. Kumar, A., Droby, S., Singh, V. K., Singh, S. K., White, J. F. (2020). Entry, colonization, and distribution of endophytic microorganisms in plants. *Microbial Endophytes*, 1–33.
35. Kumar, J., Ramlal, A., Mallick, D., Mishra, V. (2021). An overview of some biopesticides and their importance in plant protection for commercial acceptance. *Plants*, *10*(6), 1–15.
36. Kumar, L., Chhogyel, N., Gopalakrishnan, T., Hasan, M. K., Jayasinghe, S. L., Kariyawasam, C. S., Kogo, B. K., Ratnayake, S. (2021). Climate change and future of agri-food production.

In *Future Foods: Global Trends, Opportunities, and Sustainability Challenges* (pp. 49–79). Elsevier.

37. Kundan, R., Pant, G., Jadon, N., Agrawal, P. K. (2015). Plant growth promoting rhizobacteria: Mechanism and current prospective. *Journal of Fertilizers Pesticides*, *6*(2), 1–9.
38. Lata, R., Gond, S. K. (2019). Plant growth-promoting microbes for abiotic stress tolerance in plants. In *Role of Plant Growth Promoting Microorganisms in Sustainable Agriculture and Nanotechnology*. Elsevier Inc.
39. Lavania, M., Nautiyal, C. S. (2013). Solubilization of tricalcium phosphate by temperature and salt tolerant *Serratia marcescens* NBRI1213 isolated from alkaline soils. *African Journal of Microbiology Research*, *7*(34), 4403–4413.
40. Lengai, G. M. W., Muthomi, J. W. (2018). Biopesticides and their role in sustainable agricultural production. *Journal of Biosciences and Medicines*, *06*(06), 7–41.
41. Liu, Y., Xu, Z., Chen, L., Xun, W., Shu, X., Chen, Y., Sun, X., Wang, Z., Ren, Y., Shen, Q., Zhang, R. (2024). Root colonization by beneficial rhizobacteria. *FEMS Microbiology Reviews 48*(1).
42. Louden, B. C., Haarmann, D., Lynne, A. M. (2011). Use of blue agar CAS assay for siderophore detection. *Journal of Microbiology Biology Education*, *12*(1), 51–53.
43. Mącik, M., Gryta, A., Frąc, M. (2020). Biofertilizers in agriculture: An overview on concepts, strategies and effects on soil microorganisms. *Advances in Agronomy*, *162*, 31–87.
44. Mallik, B., Chakravarti, B., Chakravarti, D. N. (2016). Principles of chromatography. *Current Protocols in Essential Laboratory Techniques*, *13:6.1.1-6.1.23.*
45. Manzoor, M., Abbasi, M. K., Sultan, T. (2017). Isolation of phosphate solubilizing bacteria from maize rhizosphere and their potential for rock phosphate solubilization–mineralization and plant growth promotion. *Geomicrobiology Journal*, *34*(1), 81–95.
46. Marchin, R. M., Ossola, A., Leishman, M. R., Ellsworth, D. S. (2020). A simple method for simulating drought effects on plants. *Frontiers in Plant Science*, *10*.
47. Meier-Kolthoff, J. P., Göker, M. (2019). TYGS is an automated high-throughput platform for state-of-the-art genome-based taxonomy. *Nature Communications*, *10*(1).
48. Mercado-Blanco, J., Thomashow, L., Romanazzi, G., Prieto, C. P., Köhl, J., Kolnaar, R., Ravensberg, W. J. (2019). Mode of action of microbial biological control agents against plant diseases: relevance beyond efficacy. *Frontiers in Plant Science, 10*(845).
49. Mishra, P., Mishra, J., Arora, N. K. (2021). Plant growth promoting bacteria for combating salinity stress in plants – Recent developments and prospects: A review. *Microbiological Research*, *252*.

50. Mishra, S., Huang, Y., Li, J., Wu, X., Zhou, Z., Lei, Q., Bhatt, P., Chen, S. (2022). Biofilm-mediated bioremediation is a powerful tool for the removal of environmental pollutants. *Chemosphere*, *294*, 133609.
51. Morales-Cedeño, L. R., Orozco-Mosqueda, M. del C., Loeza-Lara, P. D., Parra-Cota, F. I., de los Santos-Villalobos, S., Santoyo, G. (2021). Plant growth-promoting bacterial endophytes as biocontrol agents of pre- and post-harvest diseases: Fundamentals, methods of application and future perspectives. *Microbiological Research*, *242*.
52. Mueller, C. W., Baumert, V., Carminati, A., Germon, A., Holz, M., Kögel-Knabner, I., Peth, S., Schlüter, S., Uteau, D., Vetterlein, D., Teixeira, P., Vidal, A. (2024). From rhizosphere to detritusphere – Soil structure formation driven by plant roots and the interactions with soil biota. *Soil Biology and Biochemistry*, *193.*
53. Mukherjee, S., Bassler, B. L. (2019). Bacterial quorum sensing in complex and dynamically changing environments. *Nature Reviews Microbiology 17*(6), 371–382.
54. Naseem, H., Ahsan, M., Shahid, M. A., Khan, N. (2018). Exopolysaccharides producing rhizobacteria and their role in plant growth and drought tolerance. Journal of Basic Microbiology 58(12), 1009–1022).
55. Nautiyal, C. S., Bhadauria, S., Kumar, P., Lal, H., Mondal, R., Verma, D. (2000). Stress induced phosphate solubilization in bacteria isolated from alkaline soils. FEMS Microbiology Letters, 182(2), 291–296.
56. Nielsen, S. S. (2017). Total Carbohydrate by Phenol-Sulfuric Acid Method. In Food Analysis Laboratory Manual, 137–141.
57. Nievola, C. C., Carvalho, C. P., Carvalho, V., Rodrigues, E. (2017). Rapid responses of plants to temperature changes. *Temperature* 4(4), 371–405.
58. Olanrewaju, O. S., Glick, B. R., Babalola, O. O. (2017). Mechanisms of action of plant growth promoting bacteria. *World Journal of Microbiology and Biotechnology*, *33*(11), 1–16.
59. Pandey, A., Tripathi, A., Srivastava, P., Choudhary, K. K., Dikshit, A. (2019). Plant growth-promoting microorganisms in sustainable agriculture. In A. Kumar, A. K. Singh, K. K. Choudhary (Eds.), *Role of Plant Growth Promoting Microorganisms in Sustainable Agriculture and Nanotechnology* (pp. 1–19). Elsevier.
60. Pang, J., Ryan, M. H., Lambers, H., Siddique, K. H. (2018). Phosphorus acquisition and utilisation in crop legumes under global change. *Current Opinion in Plant Biology*, *45*, 248–254.
61. Pantigoso, H. A., Manter, D. K., Fonte, S. J., Vivanco, J. M. (2023). Root exudate-derived compounds stimulate the phosphorus solubilizing ability of bacteria. *Scientific Reports*, *13*(1), 1–12.
62. Pathogens, precipitation and produce prices. (2021). *Nature Climate Change 11*(8).

63. Prabhu, N., Borkar, S., Garg, S. (2019). Phosphate solubilization by microorganisms: overview, mechanisms, applications and advances. In S. Meena M. Naik (Eds.), *Advances in Biological Science Research - A Practical Approach* (pp. 161–176). Academic Press.
64. Prashar, P., Kapoor, N., Sachdeva, S. (2014). Rhizosphere: Its structure, bacterial diversity and significance. *Reviews in Environmental Science and Biotechnology*, *13*(1), 63–77.
65. Rana, K. L., Kour, D., Kaur, T., Devi, R., Yadav, A. N., Yadav, N., Dhaliwal, H. S., Saxena, A. K. (2020). Endophytic microbes: biodiversity, plant growth-promoting mechanisms and potential applications for agricultural sustainability. In *Antonie van Leeuwenhoek, International Journal of General and Molecular Microbiology*, 113(8).
66. Rawat, P., Das, S., Shankhdhar, D., Shankhdhar, S. C. (2020). Phosphate-solubilizing microorganisms: Mechanism and their role in phosphate solubilization and uptake. *Journal of Soil Science and Plant Nutrition*, *21*(1), 49–68.
67. Ray, D. K., West, P. C., Clark, M., Gerber, J. S., Prishchepov, A. V., Chatterjee, S. (2019). Climate change has likely already affected global food production. *PLoS ONE*, *14*(5).
68. Richardson, A. E., Simpson, R. J. (2011). Soil microorganisms mediating phosphorus availability. *Plant Physiology*, *156*(3), 989–996.
69. Rizzo, D. M., Lichtveld, M., Mazet, J. A. K., Togami, E., Miller, S. A. (2021). Plant health and its effects on food safety and security in a One Health framework: four case studies. *One Health Outlook*, *3*(1).
70. Robert L. Tate. (2021). The soil ecosystem: Biological participants. *Soil Microbiology* (Third Edit). John Wiley Sons.
71. Sarikhani, M. R., Khoshru, B., Greiner, R. (2019). Isolation and identification of temperature tolerant phosphate solubilizing bacteria as a potential microbial fertilizer. *World Journal of Microbiology and Biotechnology*, *35*(8), 1–10.
72. Scervino, J. M., Mesa, M. P., della Mónica, I., Recchi, M., Moreno, N. S., Godeas, A. (2010). Soil fungal isolates produce different organic acid patterns involved in phosphate salts solubilization. *Biology and Fertility of Soils*, *46*(7), 755–763.
73. Shahid, M., Singh, U. B., Khan, M. S., Singh, P., Kumar, R., Singh, R. N., Kumar, A., Singh, H. V. (2023). Bacterial ACC deaminase: Insights into enzymology, biochemistry, genetics, and potential role in amelioration of environmental stress in crop plants. *Frontiers in Microbiology 14*.
74. Shariati, V. J., Malboobi, M. A., Tabrizi, Z., Tavakol, E., Owilia, P., Safari, M. (2017). Comprehensive genomic analysis of a plant growth-promoting rhizobacterium *Pantoea agglomerans* strain P5. *Scientific Reports*, *7*(1).

75. Sharma, M., Saleh, D., Charron, J. B., Jabaji, S. (2020). A crosstalk between *Brachypodium* root exudates, organic acids, and *Bacillus velezensis* B26, a growth promoting bacterium. *Frontiers in Microbiology*, *11*.
76. Sharma, S. B., Sayyed, R. Z., Trivedi, M. H., Gobi, T. A. (2013). Phosphate solubilizing microbes: sustainable approach for managing phosphorus deficiency in agricultural soils. *SpringerPlus*, *2*(587), 1–14.
77. Silva, U. C., Cuadros-Orellana, S., Silva, D. R. C., Freitas-Júnior, L. F., Fernandes, A. C., Leite, L. R., Oliveira, C. A., Dos Santos, V. L. (2021). Genomic and phenotypic insights into the potential of rock phosphate solubilizing bacteria to promote millet growth *in vivo*. *Frontiers in Microbiology*, *11*.
78. Singh, B. K., Delgado-Baquerizo, M., Egidi, E., Guirado, E., Leach, J. E., Liu, H., Trivedi, P. (2023). Climate change impacts on plant pathogens, food security and paths forward. In *Nature Reviews Microbiology*. Nature Research.
79. Singh, D., Ghosh, P., Kumar, J., Kumar, A. (2019). Plant growth-promoting rhizobacteria (PGPRs): Functions and benefits. *Microbial Interventions in Agriculture and Environment: Volume 2: Rhizosphere, Microbiome and Agro-Ecology*, 205–227.
80. Singh, D., Singh, C. K., Singh, Y. P., Singh, V., Singh, R., Tomar, R. S. S., Sanwal, S. K., Karwa, S., Mishra, V. K., Sarkar, S. K., Pal, M., Kumar, A., Yadav, R. K., Sharma, P. C. (2018). Evaluation of cultivated and wild genotypes of Lens species under alkalinity stress and their molecular collocation using microsatellite markers. *PLoS ONE*, *13*(8).
81. Singh, M. P., Singh, P., Li, H. B., Song, Q. Q., Singh, R. K. (2019). Microbial biofilms: Development, structure, and their social assemblage for beneficial applications. In *New and Future Developments in Microbial Biotechnology and Bioengineering: Microbial Biofilms Current Research and Future Trends in Microbial Biofilms* (pp. 125–138). Elsevier.
82. Sun, X., Xu, Z., Xie, J., Hesselberg-Thomsen, V., Tan, T., Zheng, D., Strube, M. L., Dragoš, A., Shen, Q., Zhang, R., Kovács, Á. T. (2022). *Bacillus velezensis* stimulates resident rhizosphere *Pseudomonas stutzeri* for plant health through metabolic interactions. *ISME Journal*, *16*(3), 774–787.
83. Tatusova, T., Dicuccio, M., Badretdin, A., Chetvernin, V., Nawrocki, E. P., Zaslavsky, L., Lomsadze, A., Pruitt, K. D., Borodovsky, M., Ostell, J. (2016). NCBI prokaryotic genome annotation pipeline. *Nucleic Acids Research*, *44*(14), 6614–6624.
84. Tecon, R., Or, D. (2016). Bacterial flagellar motility on hydrated rough surfaces controlled by aqueous film thickness and connectedness. *Scientific Reports*, *6*, 1–11.
85. United Nations. (2015). *Transforming our world: The 2030 agenda for sustainable development.*
86. United Nations. (2019). *World Population Prospects 2019: Highlights*.

87. Vurukonda, S. S. K. P., Vardharajula, S., Shrivastava, M., SkZ, A. (2016). Enhancement of drought stress tolerance in crops by plant growth promoting rhizobacteria. *Microbiological Research 184*.
88. Wan, W., Qin, Y., Wu, H., Zuo, W., He, H., Tan, J., Wang, Y., He, D. (2020). Isolation and characterization of phosphorus solubilizing bacteria with multiple phosphorus sources utilizing capability and their potential for lead immobilization in soil. *Frontiers in Microbiology*, *11*.
89. Wang, Y. Y., Li, P. S., Zhang, B. X., Wang, Y. P., Meng, J., Gao, Y. F., He, X. M., Hu, X. M. (2020). Identification of phosphate-solubilizing microorganisms and determination of their phosphate-solubilizing activity and growth-promoting capability. *BioResources*, *15*(2), 2560–2578.
90. Waraich, E. A., Ahmad, R., Halim, A., Aziz, T. (2012). Alleviation of temperature stress by nutrient management in crop plants: a review. In *Journal of Soil Science and Plant Nutrition 12*(2).
91. Wei, Y., Zhao, Y., Shi, M., Cao, Z., Lu, Q., Yang, T., Fan, Y., Wei, Z. (2018). Effect of organic acids production and bacterial community on the possible mechanism of phosphorus solubilization during composting with enriched phosphate-solubilizing bacteria inoculation. *Bioresource Technology*, *247*(August 2017), 190–199.
92. Wick, R. R., Judd, L. M., Gorrie, C. L., Holt, K. E. (2017). Unicycler: Resolving bacterial genome assemblies from short and long sequencing reads. *PLoS Computational Biology*, *13*(6).
93. Xu, Q., Ali, S., Afzal, M., Nizami, A. S., Han, S., Dar, M. A., Zhu, D. (2024). Advancements in bacterial chemotaxis: Utilizing the navigational intelligence of bacteria and its practical applications. *Science of The Total Environment*, *931*, 172967.
94. Yadav, A., Verma, P., Singh, B., Chauahan, V. S., Suman, A., Saxena, A. K. (2017). Plant growth promoting bacteria: Biodiversity and multifunctional attributes for sustainable agriculture. *Advances in Biotechnology Microbiology*, *5*(5), 1–17.
95. Yan, N., Marschner, P., Cao, W., Zuo, C., Qin, W. (2015). Influence of salinity and water content on soil microorganisms. *International Soil and Water Conservation Research*, *3*(4), 316–323.
96. Yang, P., van Elsas, J. D. (2018). Mechanisms and ecological implications of the movement of bacteria in soil. In *Applied Soil Ecology* (Vol. 129, pp. 112–120). Elsevier B.V.
97. Yasmeen, T., Ahmad, A., Arif, M. S., Mubin, M., Rehman, K., Shahzad, S. M., Iqbal, S., Rizwan, M., Ali, S., Alyemeni, M. N., Wijaya, L. (2020). Biofilm forming rhizobacteria enhance growth and salt tolerance in sunflower plants by stimulating antioxidant enzymes activity. *Plant Physiology and Biochemistry*, *156*, 242–256.
98. Zaidi, A., Khan, M. S., Ahmad, E. (2014). Microphos: Principles, production and application strategies. In M. Khan, A. Zaidi, J. Musarrat (Eds.), *Phosphate Solubilizing Microorganisms:*

Principles and Application of Microphos Technology (pp. 1–30). Springer International Publishing.

99. Zhang, J., Wang, P., Fang, L., Zhang, Q. A., Yan, C., Chen, J. (2017). Isolation and characterization of phosphate-solubilizing bacteria from mushroom residues and their effect on tomato plant growth promotion. *Polish Journal of Microbiology*, *66*(1), 57–65.
100. Zhao, J., Xie, X., Jiang, Y., Li, J., Fu, Q., Qiu, Y., Fu, X., Yao, Z., Dai, Z., Qiu, Y., Chen, H. (2024). Effects of simulated warming on soil microbial community diversity and composition across diverse ecosystems. *Science of The Total Environment*, *911*, 168793.
101. Zhou, X., Tahvanainen, T., Malard, L., Chen, L., Pérez-Pérez, J., Berninger, F. (2024). Global analysis of soil bacterial genera and diversity in response to pH. *Soil Biology and Biochemistry*, *198*, 109552. Zuluaga, M. Y. A., de Oliveira, A. L. M., Valentinuzzi, F., Jayme, N. S., Monterisi, S., Fattorini, R., Cesco, S., Pii, Y. (2023). An insight into the role of the organic acids produced by Enterobacter sp. strain 15S in solubilizing tricalcium phosphate: in situ study on cucumber. *BMC Microbiology*, *23*(1).